MSFC-291

INITIAL RESULTS FROM THE FLOATING POTENTIAL MEASUREMENT UNIT ABOARD THE INTERNATIONAL SPACE STATION

Kenneth H. WRIGHT, Jr.
CSPAR, University of Alabama-Huntsville, 301 Sparkman Dr., Huntsville, AL 35899
Phone: (256) 961-7648; Email: wrightk@uah.edu

Charles SWENSON, Don THOMPSON, Aroh BARJATYA
Utah State University

Steven L. KOONTZ
NASA/Johnson Space Center

Todd SCHNEIDER, Jason VAUGHN, Joseph MINOW
Paul CRAVEN, Victoria COFFEY
NASA/Marshall Space Flight Center

Linda PARKER
Jacobs Engineering

Them BUI
Allied Aerospace

ABSTRACT: *The Floating Potential Measurement Unit (FPMU) is a multi-probe package designed to measure the floating potential of the International Space Station (ISS) as well as the density and temperature of the local ionospheric plasma environment. The role of the FPMU is to provide direct measurements of ISS spacecraft charging as continuing construction leads to dramatic changes in ISS size and configuration. FPMU data are used for refinement and validation of the ISS spacecraft charging models used to evaluate the severity and frequency of occurrence of ISS charging hazards. The FPMU data and the models are also used to evaluate the effectiveness of proposed hazard controls.*

The FPMU consists of four probes: a floating potential probe, two Langmuir probes, and a plasma impedance probe. These probes measure the floating potential of the ISS, plasma density, and electron temperature. Redundant measurements using different probes support data validation by inter-probe comparisons.

The FPMU was installed by ISS crewmembers, during an ExtraVehicular Activity, on the starboard (S1) truss of the ISS in early August 2006, when the ISS incorporated only one 160V US photovoltaic (PV) array module. The first data campaign began a few hours after installation and continued for over five days. Additional data campaigns were completed in 2007 after a second 160V US PV array module was added to the ISS.

This paper discusses the general performance characteristics of the FPMU as integrated on ISS, the functional performance of each probe, the charging behavior of the ISS before and after the addition of a second 160V US PV array module, and initial results from model comparisons.

1 - INTRODUCTION

The International Space Station (ISS) is and will continue to be the largest structure in Earth orbit for the indefinite future. The photovoltaic (PV) solar array modules used to power the ISS operate at 160 volts with the negative side of the array tied to ISS ground. These facts along with a minimal amount of exposed conductive surface area contribute to the possibility of the ISS structure charging to significant negative voltages [1]. To mitigate the hazard that high voltages might pose to the crew on ExtraVehicular Activities (EVA) or to the surface treatments providing thermal control of the ISS structure, two Plasma Contactor Units (PCUs), developed by Glenn Research Center (GRC), were placed on the ISS preceding any installation of PV array modules.

As the first PV array module was delivered to ISS in December 2000, a plasma measurement package was delivered as well. This package, called the Floating Potential Probe (FPP) and also developed by GRC, was installed atop the Z1 truss. The GRC/FPP verified that the PCUs were controlling the floating potential of the ISS and that when the PCUs were off, the ISS did indeed charge to more negative values. The magnitude of ISS charging measured was less than expected due to lower electron collection by the PV module and due to a larger amount of ion collection surfaces than was first thought [2][3][4][5][6]. The paper by Ferguson [7] presented at this conference summarizes the results from the GRC/FPP. The GRC/FPP acquired data from December 2000 through April 2001.

As the ISS continues its build sequence, most notably with the addition of PV array modules, the need to measure ISS charging and its real-time ionospheric environment is of great importance. A total of four 160 volt PV array modules are planned for the ISS assembly complete configuration. The Floating Potential Measurement Unit (FPMU), developed by Utah State University (USU), is the follow-on plasma probe package to the GRC/FPP that will provide measurements of the ISS floating potential as well as the density and temperature of the local ionospheric plasma environment. The role of the FPMU is to provide measurements for validation of the existing ISS charging model (the Boeing/Science Applications International Corporation Plasma Interaction Model or PIM) [4] that is used in the hazard characterization and development of control processes of the vehicle and in particular for the crew when performing an EVA [8].

FPMU data acquisition must occur during time periods when the PCUs are both on and off. The FPMU data can provide a "calibration" between PCU currents and the corresponding PCU-off floating potentials that can be incorporated in the PIM. This activity allows PIM to provide accurate global characterization of hazard conditions to support hazard forecasting and contingency operations planning as ISS construction continues, without being driven to worst-case assumptions [8].

The FPMU was installed on the ISS in August 2006 and this paper provides initial results from the FPMU Data Sessions conducted during and since that time. The paper is structured as follows: a brief description of the various FPMU components is given, the data recovery process is discussed, and flight data of ISS charging behavior is illustrated. The flight data is compared to model results for both the one and two PV array module configurations of the ISS. The flight

data shown in this paper is for the PCU-off condition to focus on the PV array module collection behavior.

2 - INSTRUMENT DESCRIPTION

The FPMU is a package of four plasma instruments designed and built by USU under contract to the NASA/Johnson Space Center (JSC). Its purpose is to measure the local potential of the ISS relative to the plasma and to measure the local plasma properties of density and electron temperature. The four probes are: a Floating Potential Probe (FPP), a Plasma Impedance Probe (PIP), a Wide-sweep Langmuir Probe (WLP), and a Narrow-sweep Langmuir Probe (NLP) with associated electronics. The operation is autonomous with either an on or off state. The only control is over the operation of a heater in the WLP. Figure 1 shows a diagram of the deployed instrument with indicated dimensional data. Interference or cross-talk between the individual instruments of the FPMU was a concern. Distances between the probe surfaces have been set to avoid overlapping sheaths. The FPMU has been described elsewhere [9][10][11] but a brief description of each probe is given below.

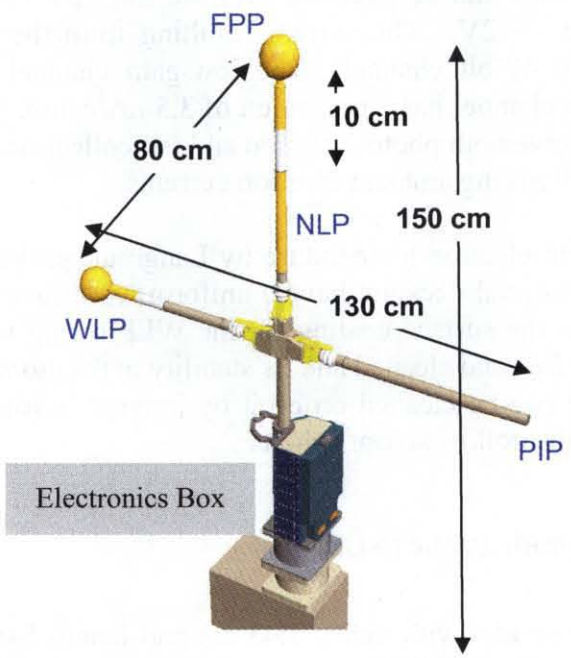

Figure 1 - Diagram of FPMU in its deployed state with indicated dimensions.

2.1 - Floating Potential Probe (FPP)

The FPP is a gold-plated sphere of radius 5.08 cm. The sphere is isolated from chassis ground by a high impedance circuit, approximately 10^{11} Ω. The sphere "floats" at a floating potential determined by local plasma conditions, which is within a few kT_e of the plasma potential and provides a good reference for measuring the potential of the ISS (k = Boltzmann's constant and T_e = electron temperature). Data is sampled as a 12-bit word with 100 mV resolution. The FPP is sampled at 128 Hz.

2.2 - Wide-Sweep Langmuir Probe (WLP)

The WLP is a gold-plated sphere of radius 5.08 cm. A voltage sweep from –20 V to 80 V relative to chassis ground, ISS structure, is applied to the probe, and the resulting currents to the probe are measured. Sweeps are accomplished each second, with the potential sweeping from low to high voltage in one second and back down from high to low in the next second. The sweep is comprised of three parts: steps of ~ 250 mV from –20 V to 0 V, steps of ~ 25 mV from 0 V to 50 V, and steps of ~ 250 mV from 50 V to 80 V. This pattern was chosen as a balance between available telemetry space and the amount of data necessary to derive the required parameters. The small step size from 0 V to 50 V provides sufficient resolution for a determination of Te (which requires several samples in the electron retarding portion of the sweep). The floating potential can be obtained over the full –20 V to 80 V range, within the uncertainty requirement of +/- 2V. The current resulting from the applied voltage sweep is measured on two different 12-bit channels. The low-gain channel has a resolution of 700 nA/count and the high gain channel has a resolution of 3.5 nA/count. The high-gain channel has sufficient sensitivity to observe both photo emission and ion collection currents whereas the low-gain channel is suited for observing ambient electron currents.

Measurement of ionospheric electron temperature by Langmuir probes is subject to significant error if the probe surface material does not have a uniform work function, or if the probe is not clean. Gold was chosen as the surface coating for the WLP owing to its nearly uniform work function when properly applied and cleaned and its stability in the atomic oxygen environment of low Earth orbit. The WLP can be cleaned on orbit by internal heating through activation of a small halogen lamp inside the hollow sensor sphere.

2.3 - Narrow-Sweep Langmuir Probe (NLP)

The NLP is a gold-plated cylinder with radius 1.43 cm and length 5.08 cm. The NLP is placed mid-way on the boom supporting the FPP. The probe surface of the NLP is surrounded on each side by a gold-plated guard cylinder with radius 1.43 cm and length 10.2 cm, which are swept in synchrony with the NLP. A sweep from – 4.9 V to + 4.9 V, in steps of ~12 mV, is applied to the NLP during one second, followed by a sweep down from 4.9 V to – 4.9 V in the next second. This sweep voltage is referenced to the floating potential measured by the FPP. Hence, even though the sweep range of the NLP is small compared to the possible range of ISS potentials, the electron and ion retarding regions of the plasma current-voltage profile will be seen, as the

region sampled will move through the – 180 V to + 180 V range of the FPP to match the current conditions. This configuration will allow the density and electron temperature to be determined at 1 Hz. In addition, the ISS potential measured by the FPP will be verified, since if it is incorrect, the NLP will not be referenced to the proper potential and the transition from ion collection to electron collection will not be seen in the +/- 4.9 V sweep.

The current resulting from the applied voltage sweep is measured on two different 12-bit channels. The low-gain channel has a resolution of 87.5 nA/count and the high gain channel has a resolution of 0.44 nA/count. Like the WLP, the high gain channel has sufficient sensitivity to observe both photo-emission and ion saturation currents where as the low-gain channel is suited for observing electron currents. The surface of the NLP is gold for the same reason as the WLP, the desire for a uniform work function and stability in atomic oxygen. However, there is no heating lamp within the NLP, so there is no active cleaning mode for this probe.

2.4 - Plasma Impedance Probe (PIP)

The PIP consists of a short dipole antenna electrically isolated from the ISS. The dipole is normally oriented perpendicular to the ram flow direction and away from the ISS wake. The PIP measures the electrical impedance (magnitude and phase) of the antenna at 256 frequencies over a 100 KHz to 20 MHz range. Electron density, electron-neutral collision frequency, and magnetic field strength can potentially be deduced from these impedance measurements. The PIP will also track the frequency at which an electrical resonance associated with the upper-hybrid frequency occurs using a technique known as the Plasma Frequency Probe (PFP). From this resonance the absolute plasma density can be determined at a 512 Hz rate with great accuracy. Although not formally required by NASA, the PIP was added to the FPMU instrument suite per agreement between USU and NASA.

Table 1 summarizes the performance of the FPMU instruments to measure the ISS floating potential, V_F, the local plasma density, N, and electron temperature, Te.

Table 1 - The measured parameters, rates, and effective ranges for the FPMU.

Sensor	Measured Parameter	Rate (Hz)	Effective Range
FPP	V_F	128	-180 V to +180 V
WLP	N T_e V_F	1	10^9 m^{-3} to $5{\cdot}10^{12}$ m^{-3} 500 K to 3000 K -20 V to 80 V
NLP	N T V_F	1	10^9 m^{-3} to $5{\cdot}10^{12}$ m^{-3} 500 K to 3000 K -180V to +180 V
PIP	N_e	512	$1.1{\cdot}10^{10}$ m^{-3} to $4{\cdot}10^{12}$ m^{-3}

3 - FLIGHT OPERATIONS

The FPMU was carried to the ISS on STS-121 in July 2006. On August 3, 2006, it was installed on external camera port 2 at the end of the S1 truss during an EVA performed by Jeff Williams and Thomas Reiter. The FPMU interface is with the TV Camera Interface Controller (TVCIC) which is attached to a camera stanchion that places the FPMU a few meters above the S1 truss surface. The FPMU makes use of the TVCIC interface for power and formats its data as a video signal for Ku-band transmission to the ground. Details of how the FPMU integrates its data with the ISS video system can be found in Swenson et al. [9].

Figure 2 shows a picture of the FPMU as installed on the ISS. While the crew members returned to the airlock to obtain additional items for other EVA activities, the instrument was powered-on briefly for 15 minutes to confirm proper integration At approximately GMT 215/23:00 the FPMU was powered on and remained powered until approximately GMT 220/14:00.

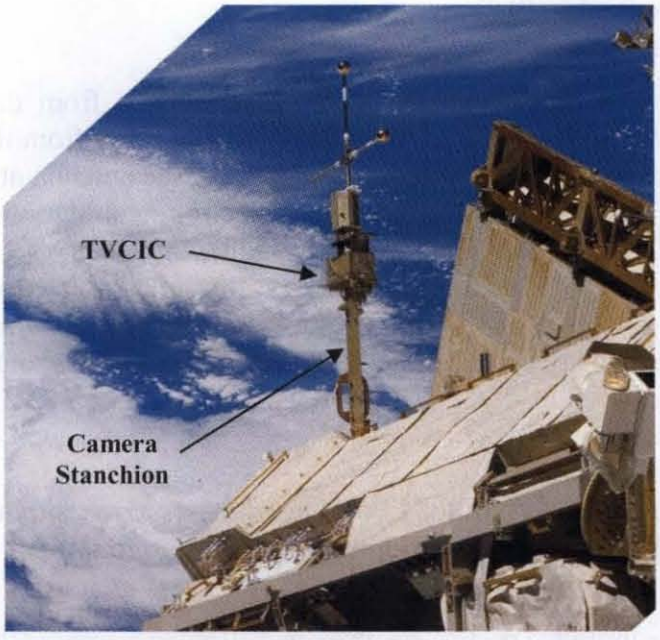

Figure 2 - FPMU as installed on the starboard S1 truss.
(Modified NASA photo S116E06645)

The FPMU telemetry is routed to a workstation located in the Mission Control Center building at JSC. The workstation shows a real-time display of key values from each 1-second telemetry frame as well as archives the data. In June 2006, the data path through JSC was verified by flowing FPMU Functional Test data through the system. Beginning with the flight data in August 2006, the telemetry as captured by the workstation is marred by noise. Each telemetry frame is divided into 7 sections and a checksum value calculated for each section. For perfect data capture, checksums calculated by the workstation for each telemetry frame would agree with those calculated on orbit and stored in the telemetry. A checksum value = 0 for the whole telemetry frame implies complete agreement between the values calculated on orbit and those calculated on the ground. Checksum values can be in the range 0 to 7 to indicate degrees of

telemetry frame corruption. For example, Fig. 3 shows a histogram of the checksum values for all of day 2006/217. Only about 10% of the telemetry frames received had checksums equal to 0 for the August 2007 Data Session. Some limited troubleshooting has been performed to isolate where the noise is introduced, but nothing definitive has been determined at the writing of this paper. To the FPMU's advantage, the video system provides a unique high bandwidth channel for its data. As will be discussed in Sections 3.1 – 3.3, the large volume of data per telemetry frame (6,776 16-bit words) can be filtered and smoothed to recover the vast majority of it.

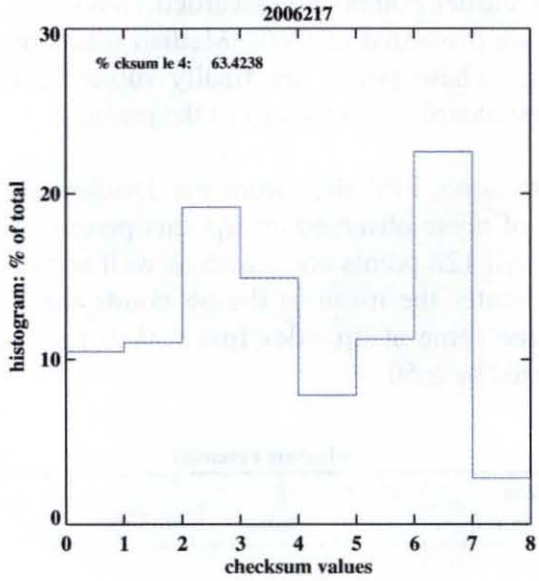

Figure 3 - Histogram of the checksum values for day 2006/217. A checksum value = 0 designates uncorrupted data for a telemetry frame.

Table 2 contains a list of the days for 2006 and 2007 to-date that the FPMU was powered and transmitted data. The Ku-band downlink from the ISS is not continuous. For the August 2006 Data Session, the Ku-band efficiency (percentage of received transmissions relative to the total FPMU operation time) was in the range of 45% - 50%. For the 2007 Data Sessions to-date, the Ku-band efficiency is close to 60%. Additional Data Sessions are planned in 2007 and 2008.

Table 2 - FPMU Operation Days.

Year	GMT Day	Calendar Day
2006	215 - 220	Aug. 3-8
2007	022 - 030	Jan. 22 - 30
	060 - 062	Mar. 1 - 3
	103 - 104	Apr. 13 - 14
	123	May 3

3.1 - FPP data processing

The straightforward approach to analyzing FPP data is to simply find the mean (fpv) and standard deviation (fp_vdev) of the 128 sample points. However, the noise present in the telemetry frame causes the mean and standard deviation to fail an acceptance test of $|fp\_vdev/fpv| \leq 0.10$. Examining the values of the FPP measurements in many telemetry frames shows that the noise is basically "salt-and-pepper"-type (bit shifts) that can be easily eliminated and/or smoothed. Based on the location of the FPMU and the ISS flight attitude, FPP values of < -10 V can be considered as outlier points and discarded. Values $> +150$ V are considered as outliers for this polarity and are discarded as well. Median filters of various widths are applied to the remaining data points. These points are finally subjected to an iterative process that excludes values that are $> 2\sigma$ standard deviations from the mean.

To illustrate the analysis technique, FPP data from the January 2007 Data Session is chosen because of the large amount of noise observed during this period. Figure 4 shows data from a one-second FPP acquisition. All 128 points are shown as well as the -10 V and 150 V exclusion boundaries. The red line indicates the mean of the 66 points that survive the algorithm. The acceptance criteria remains the same at $|fp\_vdev/fpv| \leq 0.10$ and an additional criteria of the number of surviving points must be ≥ 50.

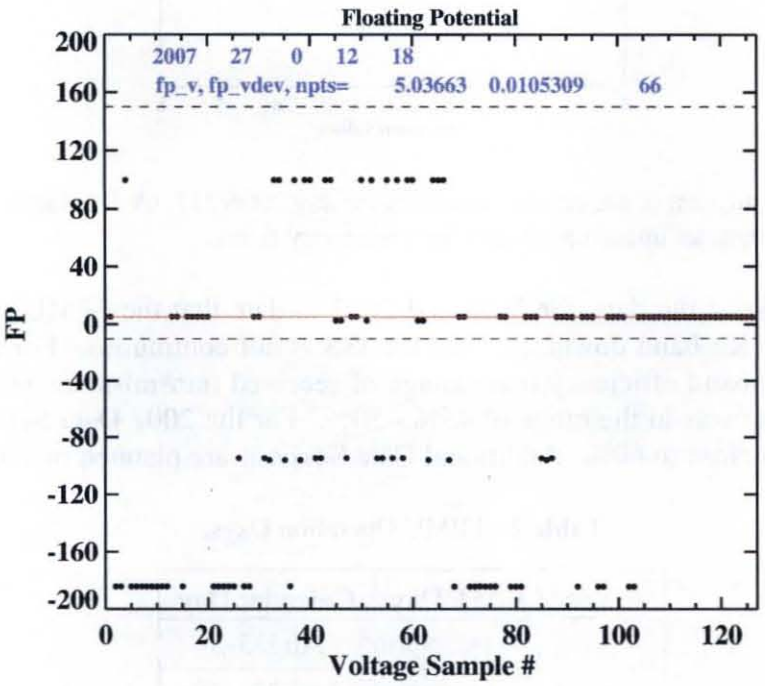

Figure 4 - Example of FPP analysis of data from 2007/027/00:12:18.

Recovery rates for the FPP data are: (1) August 2006 > 99% per day; (2) January 2007 > 90% per day; (3) March 2007 > 98% per day; (4) April 2007 > 98% per day; and (5) May 2007 > 98% per day.

3.2 - WLP and NLP data processing

The initial approach to recovery of the plasma properties from the WLP and the NLP current-voltage characteristic is through the so-called "graphical method". In this method, the different regions of the probe characteristic, i.e., the ion saturation region, the electron retarding region, and the electron saturation region, are treated separately (see call-outs in Fig. 5a). This approach was recently used by Lebreton et al. [12] to process data from the Detection of Electro-Magnetic Emission Transmitted from Earthquake Regions (DEMETER) satellite Langmuir probe. Because of the existence of noise in the FPMU telemetry frame, various filtering techniques must be performed as each region of the probe characteristic is analyzed.

The basic relationships between voltage and current in the different regions for the data processing are given below. For the ion saturation region, a linear dependence of current (I_i) as a function of applied probe voltage (V) is assumed:

$$I_i = a_1 + b_1 \cdot V, \qquad \textbf{[1.]}$$

where a_1 and b_1 are determined from curve-fitting. For the electron retarding region, a Boltzmann relation (Maxwellian electrons) is assumed for the electron current I_e:

$$I_e = I_{eo} \exp[q(V-V_{sp})/kT_e], \qquad \textbf{[2.]}$$

where q = electron charge 1.609×10^{-19} coulombs; k = Boltzmann's constant 1.38×10^{-23} joules/K; V_{sp} = plasma space potential; T_e = electron temperature; and I_{eo} = the random electron thermal current given by

$$I_{eo} = \tfrac{1}{4}\, q\, N_e\, A_p\, (8kT_e/\pi m_e)^{1/2}, \qquad \textbf{[3.]}$$

where N_e = electron density; A_p = area of probe; and m_e = electron mass = 9.1×10^{-31} kg. Equation [2] can be re-written as

$$\log_{10} I_e = a_2 + b_2 \cdot V, \qquad \textbf{[4.]}$$

where a_2 and b_2 are determined from curve-fitting. Note that b_2 is the slope of the data in semi-log space and is proportional to $1/T_e$. For the electron saturation region, the current is estimated as a second order polynomial

$$I_e = a_3 + b_3 \cdot V + c_3 \cdot V^2 , \qquad \textbf{[5.]}$$

where a_3, b_3, c_3 are determined from curve-fitting. Further discussion about the electron saturation region occurs later in this section.

The basic steps in the analysis routine are as follows:

1. Find the floating potential (V_F) by locating the voltage at which the current changes polarity. The polarity of the measured current for each probe is the "Langmuir

convention" where ion current is recorded as negative and electron current is recorded as positive.

2. Correct for photoelectron current, I_{ph}. For the spherical WLP, this is a constant value of $I_{ph} = 29\ \mu A/m^2 \cdot$ WLP-cross-section $= 0.24\ \mu A$. For the cylindrical NLP, I_{ph} depends on the sun-angle relative to the probe axis, i.e., $I_{ph} = 29\ \mu A/m^2 \cdot$ NLP-cross-section $\cdot \sin\theta_S = 4.21 \times 10^{-2}\ \mu A \cdot \sin\theta_S$, where θ_S is the angle between the NLP-sun vector and the FPP mast axis.
3. Isolate a region of the ion saturation current more negative than the floating potential and curve-fit to Eq. [1].
4. Subtract the ion current baseline as determined by the fit to Eq. [1] to derive the electron-only current.
5. Obtain the first derivative of the electron current and locate the voltage at which a maximum occurs in the derivative. This voltage serves as the initial estimate of the space potential, V_{sp} .
6. Based on the value of V_{sp} select a range of voltage more negative than V_{sp} but more positive than V_F to capture the electron retardation region. The logarithm of the electron current in this selected voltage range is curve-fit to Eq. [4], i.e., a linear fit in semi-log space.
7. Select a range of voltage a few volts more positive than the estimate for V_{sp} and curve-fit these points to Eq. [5].
8. Solve for a new V_{sp} through the intersection of curves determined from the curve-fits of Steps (6) and (7).
9. Use the new V_{sp} and perform one iteration by repeating Steps (6) – (8).

The plasma properties are determined in the following manner for each Langmuir probe. The ion current from Eq. [1] is evaluated at the space potential and assumed to be the ion ram current since the probes are in the mesothermal flow regime, i.e., electron thermal speed > ISS speed > ion thermal speed, and the dominant ion at ISS altitude is O^+. The ion ram current to the probe is given by

$$I_{ram} = q \cdot N_i \cdot V_{ISS} \cdot A_{LP}, \qquad \textbf{[6.]}$$

where q = electronic charge, N_i = ion density, V_{ISS} = magnitude of the ISS velocity, and A_{LP} = cross-section of the probe. For the spherical WLP, the cross-section is a constant value. For the cylindrical NLP, a cosine of the angle between the probe normal and velocity vector must also be included. The **ion density** is found by inverting Eq. [6]. The **electron temperature** (in Kelvin) is derived by using the slope from the curve-fit to Eq. [4] in the relation

$$T_e\,(K) = (q \cdot \log_{10}e) / (k \cdot b_2) = 5042 / b_2. \qquad \textbf{[7.]}$$

The **electron density** is found by inverting Eq. [3], using the T_e value from Eq. [7], and using the measured electron current at V_{sp}. The **floating potential** and **space potential** are determined from Steps (1) and (9) in the analysis routine.

To illustrate the Langmuir probe data processing, an analysis of a single WLP and NLP voltage-current curve for each probe for a common time is featured. Figure 5 shows the WLP result

while Fig. 6 shows the NLP result. Part (a) of each figure shows the absolute value of total current to illustrate the region used for analysis. Part (b) of each figure shows the ion saturation current region and the linear fit represented in red. Part (c) shows the first derivative of the electron current. The vertical dashed line indicates the voltage at the maximum derivative which serves as the initial estimate of the space potential. Part (d) in each figure shows the curve-fits (in red) to the electron retarding and electron saturation regions. The horizontal dashed lines indicate the region of current over which the electron temperature is determined. This region is greater than one $\log_{10}$ decade in current. The derived plasma properties are noted at the base of each figure. The good agreement between the corresponding values from each probe for this one example time is noted here but is demonstrated over long time periods in Section 4.

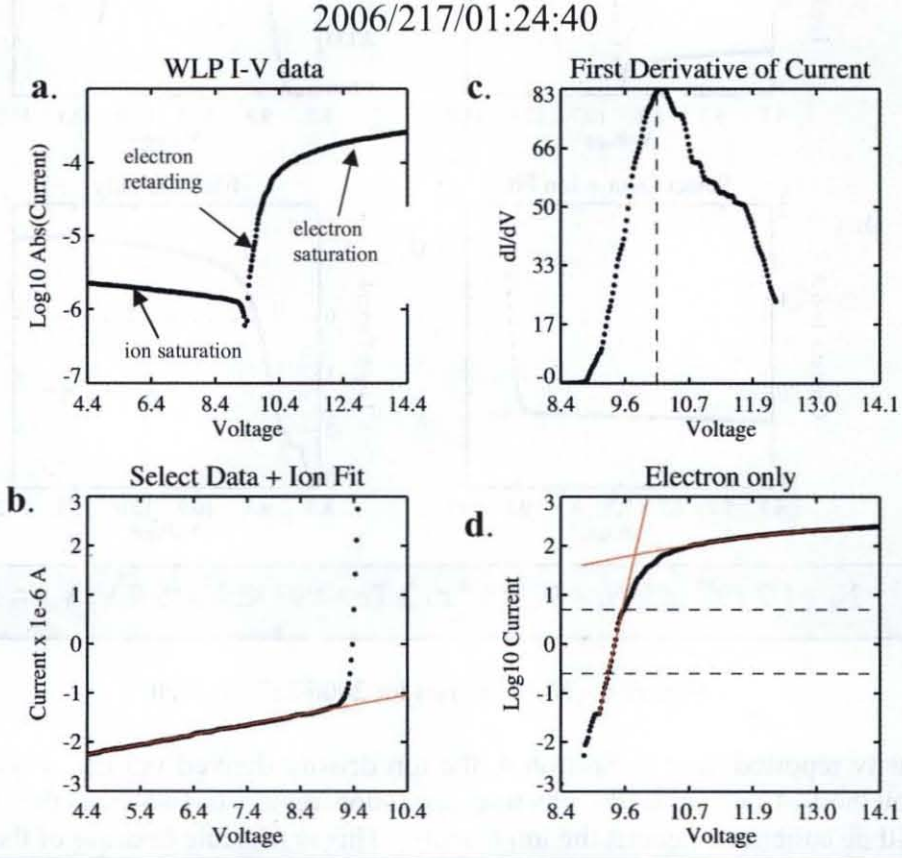

Figure 5 - WLP analysis for 2006/217/01:24:40.

It is noted that the derived electron density and ion density differ by approximately a factor of 2 for this example. At other times, better agreement between the ion and electron density is found. Consistency in agreement throughout the data set may be expected to improve when a more rigorous theory is applied to the electron saturation region rather than the initial approach of a simple second-order polynomial. The sizes of the WLP and NLP are such that each probe radius is larger than the Debye length and of the same order as the electron gyro-radius. The Orbit-Motion-Limited expression for the electron saturation region is not applicable. Application of

detailed probe theories is underway (ex. [13] [14] [15]). However, initial results show that a single theory does not give a consistent answer. A future paper will discuss this work.

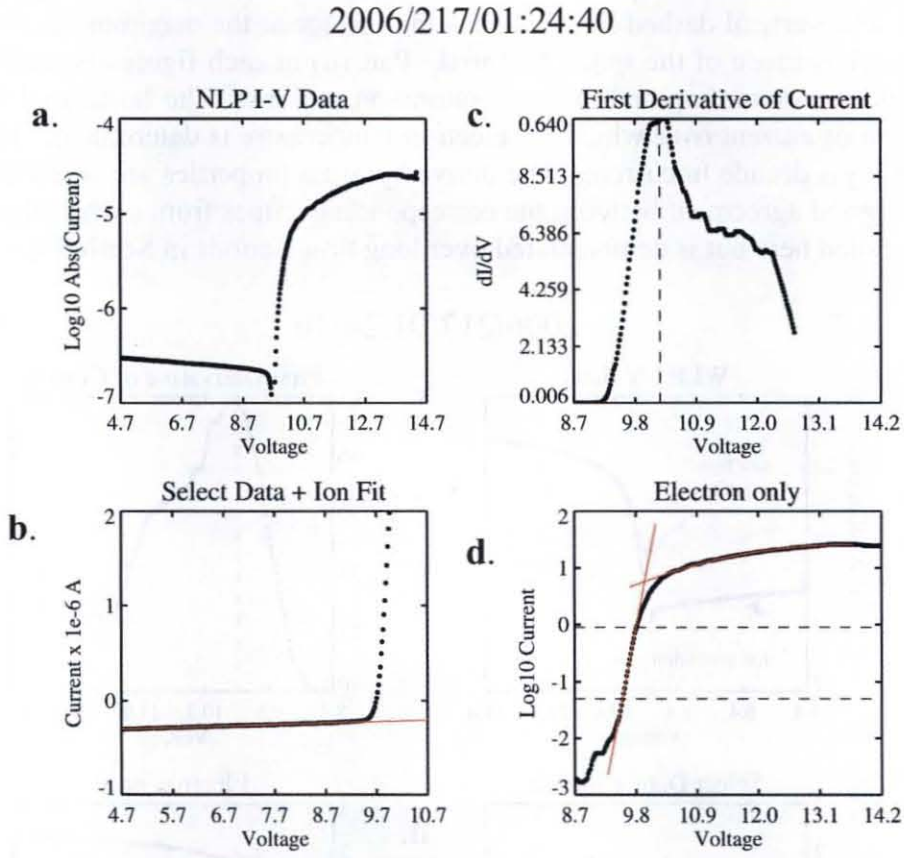

Figure 6 - NLP analysis for 2006/217/01:24:40

For the density reported later in Section 4, the ion density derived via Eqs. (1) and (6) is used. When the method of analyzing the electron saturation region is finalized, the derived electron densities will be calibrated against the ion density. This is possible because of the design of both the WLP and NLP - the sweeps are both bipolar in current and voltage. This calibration of electron density to ion density in Langmuir Probe data reduction was used by Brace for many years in processing his experiment data from orbiting cylindrical probes [16].

For the examples shown here, the electron retarding region for each probe is observed to be linear over approximately two decades in this semi-log presentation. Most of the time agreement between the two probes lies in the range of 10% - 20%. At the beginning of each FPMU Data Session, the WLP heating lamp is operated for one orbit. Minimal (if any) hysteresis has been observed on the WLP or even on the non-heated NLP probe. The lack of hysteresis and the fact that sub-1000 K temperatures are observed simultaneously on each probe indicates that very little contamination exists on the probe surfaces.

As mentioned at the beginning of Section 3, each telemetry frame has a checksum value associated with it that indicates data quality or "noise" level. It is observed that the scatter on the electron temperature data is reduced by only accepting the values from telemetry frames that have checksum ≤ 4. With this criteria, LP recovery rates from the August 2006, March 2007, April 2007, and May 2007 Data Session lie in the range of 45% - 65%. Recovery of LP data from the January 2007 Data Session is minimal (< 10%) because of an unusual amount of noise.

3.3 - PIP data processing

As mentioned earlier, the PIP consists of two operational components: a 512-point tracking circuit (PFP) and the 256-point frequency sweep where the impedance (magnitude and phase) are measured. The PIP components of the FPMU were late additions into an already compressed hardware delivery effort (14 months). Complete satisfaction in the PIP operational aspects could not be achieved before FPMU delivery. As a consequence, the PFP only rarely is able to lock-in on the proper frequency and yield meaningful data. However, the results are better for the impedance sweep data. An example of good data from the frequency sweep is shown in Figs. 7a and 7b. The horizontal line in Fig. 7a indicates the 0-deg phase location. The vertical line in Fig. 7a indicates the frequency at which the phase crosses the 0-deg level for the second time. This frequency should be the upper hybrid frequency [17] [18]. The inability to consistently track also affects the phase versus frequency measurement such that the phase is shifted and no second-zero phase crossing occurs for most of the time. The magnitude versus frequency variation, shown in Fig. 7b, always has a peak and the frequency location of this peak can be used as a 1st-order approximation for the upper hybrid frequency. A more rigorous analysis would fit a detailed probe response equation to this data [19] but for our initial PIP data recovery only the location of the peak in the magnitude versus frequency data is used.

From cold plasma wave theory, the upper hybrid frequency (f_{uh}) is a combination of the plasma frequency and the cyclotron frequency and is given by

$$f_{uh}^2 = f_p^2 + f_c^2 , \qquad \textbf{[8.]}$$

where f_p = plasma frequency = $(1/2\pi)(4\pi Nq^2/m_e)^{1/2}$,
f_c = electron cyclotron frequency = $qB/2\pi m_e = 2.8 \times 10^6$ B(gauss) Hz,
N = plasma density, q = electron charge, m_e = electron mass, and B = magnetic field.
Solving Eq. [8] for density gives:

$$N(m^{-3}) = 1.24 \times 10^{-2} [f_{uh}^2 - f_{ce}^2] . \qquad \textbf{[9.]}$$

The electron cyclotron frequency is calculated from the International Geomagnetic Reference Field model (http://www.ngdc.noaa.gov/IAGA/vmod/) using the ISS orbit track information. The validity of the application of cold plasma wave theory to the ionosphere has been discussed in Ward et al. [20].

A comparison of the PIP-derived electron density with the WLP-derived ion density is shown in Fig. 7c for the first hour of 2006/217. Agreement between the probes can be seen to be quite good thereby justifying the use of the LP-derived ion densities discussed in Section 4. The PIP

data shown in Fig. 7 is from all telemetry frames regardless of checksum value. Most of the scatter can be eliminated by only analyzing PIP data from telemetry frames where the checksum ≤ 4. Only a small part of the PIP data from the FPMU data sessions has been analyzed to-date but the method outlined here holds promise for good data recovery.

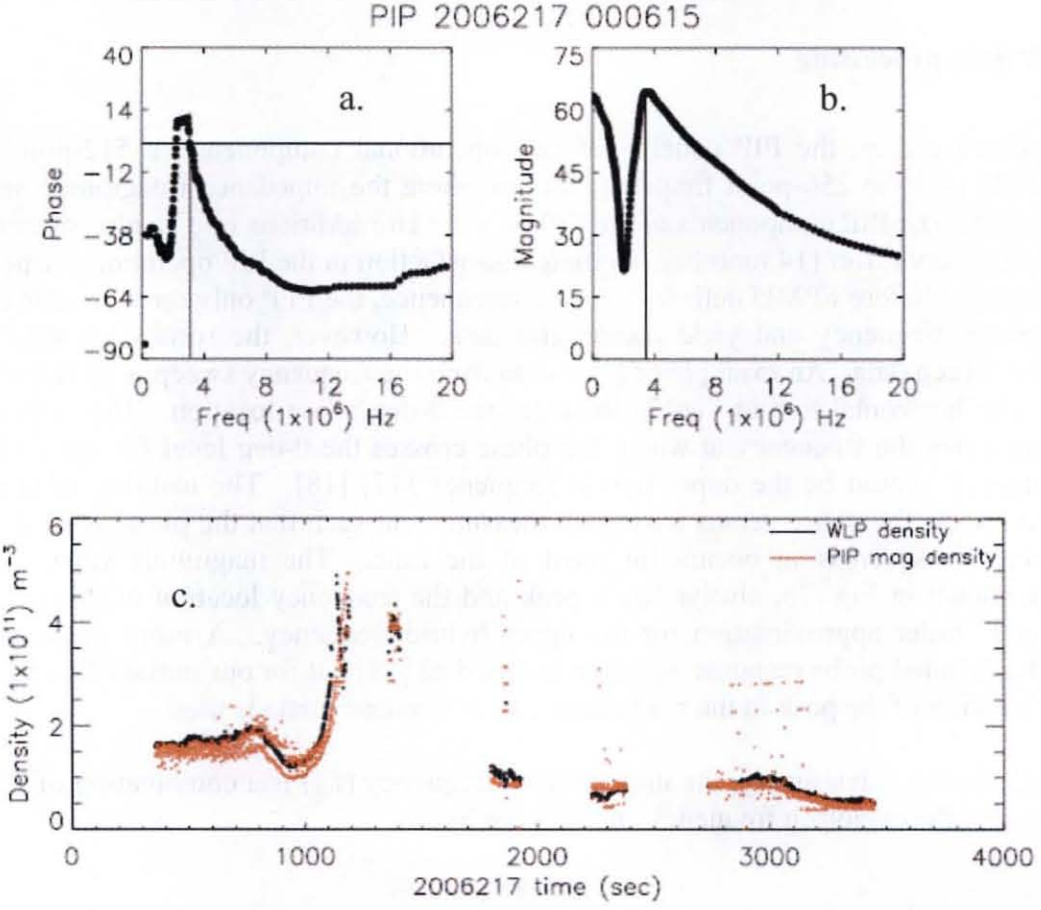

Figure 7 - PIP data from 2007/217. (a) One-second data for phase versus frequency. (b) One second data for magnitude versus frequency. (c) One hour of PIP-derived density compared to the WLP ion density.

4 - ISS CHARGING

In examining the charging of the ISS, the most important element to note is the number of PV array modules – the charging is dominated by the electron collection on the PV array. In August 2006 when the FPMU was installed, the ISS had only one PV array module (see Fig. 8). Each PV array module consists of two wings with each wing consisting of two panels. As mentioned in Section 1, this PV array module was installed on the ISS in December 2000. So the FPMU is acquiring data on the same PV array module that the GRC/FPP had "diagnosed" in early 2001. Although the starboard and port truss segments, with its predominantly anodized surfaces, were

the largest hardware addition to the ISS during the 2001 to 2006 time period, the number of PV array modules remained the same and the Russian segment configuration remained the same. The Russian segments are important to the final charging level in that their surfaces provide the area for ion collection [21] [22]. The model used to forecast ISS charging had its genesis during the GRC/FPP operational period in 2001 and was tailored to capture all of the charge collecting on the exposed conductive surfaces at that time. The FPMU data from 2006 can be used as validation of the model.

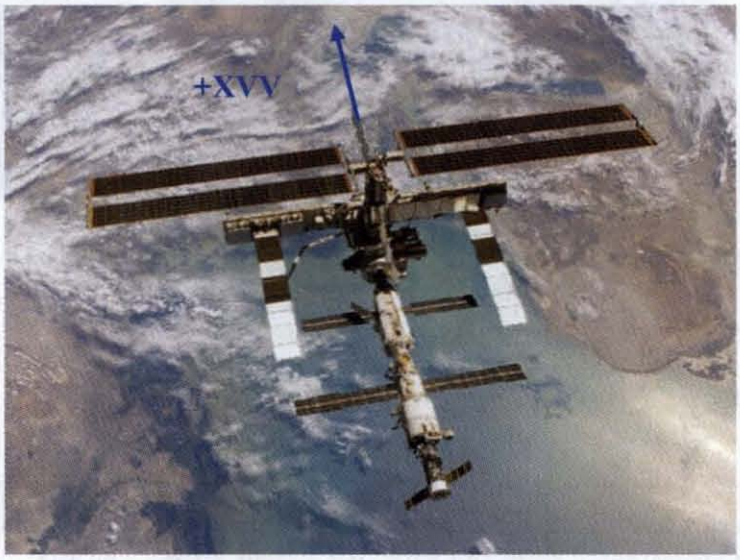

Figure 8 - ISS configuration and nominal flight attitude during the August 2006 FPMU Data Session.

It was important that the FPMU acquire data in August 2006 because a second PV array module was carried to the ISS on the STS-115 mission and installed in September 2006. One of the wings of the original PV array module was retracted during the STS-116 mission to the ISS in December 2006 and the power system was rewired such that the second PV array module was made operational. Figure 9 shows a picture of the ISS configuration for the 2007 FPMU Data Sessions to-date. The purpose of the 2007 FPMU data is to assess if the collection properties of the new PV array module are the same as the original module. As seen in Fig. 9, only three wings out of the possible four are deployed and two of those are new.

In the remainder of this section, data from the various FPMU instruments are presented and compared with the results from the ISS charging model - PIM. PIM development was a joint collaboration between Science Applications International Corporation (SAIC) and Boeing to capture all of the appropriate current collection features of the various ISS elements [23] [4] [24] [21]. These items include the PV arrays, the PV array masts which are conducting wires, and the conducting part of the ISS structure which is predominately the Russian segments. The Russian segments are covered by thermal blankets that have grounded, conducting wires embedded in them. SAIC developed the analytical expressions for charged particle collection while Boeing integrated this with the vehicle aspects such as the amount of solar array area, the power management of the array strings, attitude of the arrays, etc.

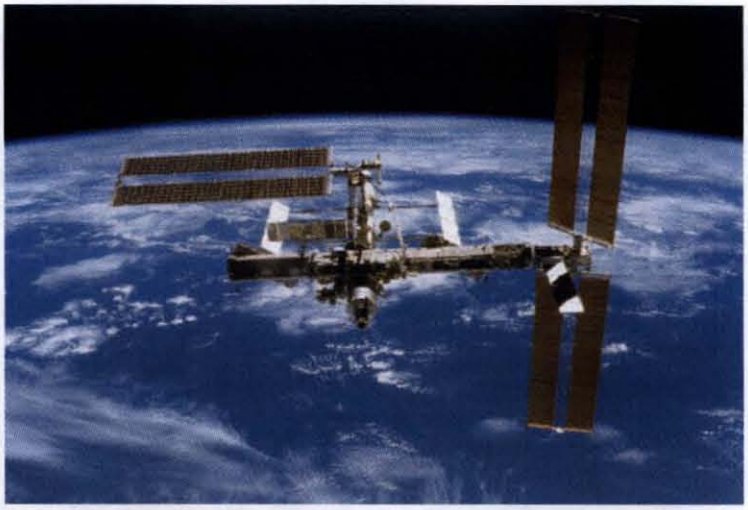

Figure 9 - ISS configuration during the 2007 FPMU Data Sessions to-date.
The +XVV attitude is basically out of the page.

4.1 - 2006/217 data

Figure 10 (on page 20) contains a summary plot of FPMU data for an orbit on day 2006/217. There is no time-series averaging for the FPMU data presented here. The top panel contains floating potential measurements from the FPP, WLP, and NLP. The ISS charges negative with respect to the plasma but the floating potential is graphed as a positive number here. The middle and bottom panels show the density and electron temperature, respectively, as determined from the WLP and NLP. The floating potential variation with time illustrates the three types of charging that the ISS experiences: (1) a $V_{ISS}xB\cdot\ell$ background variation due to the motion of the large ISS structure through the Earth's magnetic field; (2) charging when the ISS moves out of the Earth's shadow and into sunlight (eclipse exit); and (3) charging during passage through the equatorial region where the Equatorial Ionization Anomalies (EIA) or Appleton anomalies exist. The ISS attitude during this timeframe is nominally where the +X-axis is pointed into the velocity vector (defined as +XVV and noted in Fig. 8). Recall that the FPMU is mounted on the starboard side so that with this flight attitude and the orbit motion, significant $V_{ISS}xB\cdot\ell$ values occur near the maximum northern latitude of the ISS orbit.

During the August 2006 Data Session, the night-to-day transition occurred near the maximum northern latitude yielding an ~ 25 V floating potential that was the sum of a $V_{ISS}xB\cdot\ell$ level (~ 10 V) and the eclipse exit charging (~ 15 V). The value of 25 V was the maximum floating potential observed by the FPMU during the August 2006 data acquisition. At eclipse exit, all of the strings are in the array circuit such that when the cells are illuminated, they produce their integrated positive voltage relative to the plasma. The ionospheric electrons are collected on each cell edge due to this positive sheath. Since the full power developed by the array is not needed by the ISS, some of the strings are shunted – they are not connected to ISS ground resulting in fewer ionospheric electrons flowing to the ISS structure. The duration of charging

above the $V_{ISS}xB\cdot\ell$ background is determined mostly by the array management profile but also by the local plasma conditions.

The sensitivity of charging due to local plasma conditions is best illustrated by the passage of the ISS through the equatorial ionosphere. Duration of the charging above the $V_{ISS}xB\cdot\ell$ background exists from approximately hour 1.85 to hour 1.95 while most of the PV array is shunted. During these few minutes, the density exhibits a marked increase but more importantly, the electron temperature shows a local minimum (see the thin vertical lines drawn across the panels). This sensitivity of charging with respect to electron temperature was observed in the GRC/FPP data from early 2001 [25] [5] and was accommodated in the PIM development [23]. The physical reason for this behavior is that the lower temperature environment contains more electrons that are below the energy and angular momentum threshold to execute a trajectory through the gap between the solar array cells and strike the cell edge [5].

In general, good agreement is obtained between data from the various FPMU probes. The floating potential data are basically identical from the three probes. An occasional deviation between the ion density derived from the WLP and the NLP is observed. The NLP is a cylindrical probe and extraction of the ion density from the ion saturation current depends on accurate knowledge of the ram angle, i.e., the angle between the probe axis and the ram velocity. A nominal, constant ram angle has been used in the processing of the NLP data for this plot but it is known that the ISS can drift about its programmed attitude within certain dead-bands. The agreement between the WLP and NLP for electron temperature is in the 10 % - 20% range. The scatter in the data is due to noise in the telemetry frame. The NLP has less scatter due to its smaller voltage step-size in the electron retarding region. For cylindrical probes like the NLP, the angle between the probe axis and the magnetic field can influence the collected current behavior. The behavior of the NLP electron temperature at hour 1.8 may be due to magnetic field effects.

Also included in Fig. 10 are the predictions from PIM. The plasma environment input to PIM is the International Reference Ionosphere-IRI-2001. Information on IRI-2001 may be obtained from the following website http://modelweb.gsfc.nasa.gov/models/iri.html. The PIM result for the nominal or 0-sigma IRI-2001 input is denoted by the solid line in each of the three panels. PIM results for variations on the nominal IRI-2001 are included as well. The sense (positive or negative) of the variation is defined by its influence on the PIM result. A positive sigma (denoted by the dashed line) is defined as PIM predicting a larger charging value which requires a relatively higher density and lower temperature. A negative sigma (denoted by the dotted line) is defined as PIM predicting a lower charging value which requires a relatively lower density and higher temperature. The quantitative difference in the three IRI-2001 cases is shown in the middle and lower panels of Fig. 10. The numerical factors to modify the nominal IRI-2001 to the +1-sigma and –1-sigma standard deviation cases were determined as follows [26] [27]. Plasma data from the Atmospheric Explorer-C, Atmospheric Explorer-D, and Dynamics Explorer-2 satellite databases were sorted for simultaneous (N,T_e) pairs for appropriate ISS altitude and latitude ranges for daytime conditions. For each pair of (N,T_e) data values, the corresponding IRI-2001 values are computed. From scatter plots of N(data)-vs-N(IRI-2001) and Te(data)-vs-Te(IRI-2001), representations of the ±1, ±2, and ±3-sigma variances of each property are determined. For ISS hazard forecasting, PIM has been used with this type of

variation on the plasma model input [6] [21]. A utility of the FPMU plasma data is to corroborate or to modify the variance boundaries.

The PIM predictions of floating potential generally capture the behavior of the measured data but there is an apparent shift in the location of the predicted eclipse exit charging. This shift has nothing to do with the current collection aspects of PIM but in the way the night-day transition is determined. At the time of the writing of this paper, the ISS sun sensor data is used to determine the eclipse exit time. However, it is known that the sun sensor at eclipse exit has a delay of up to a few minutes relative to the time that the PV arrays "sense" the sun and provide full power. (R. Mikatarian, private communication). A modification to PIM is underway at this time to use another measurement to mark the eclipse exit event. The item to focus on is the predicted magnitude of the eclipse exit floating potential. The +1-sigma case almost quantitatively matches the FPMU measured value – the difference is < 1 V.

The sensitivity of the charging with electron temperature is further demonstrated by examining the eclipse exit and the equatorial region charging events. The 0-sigma IRI-2001 density at hour 1.5 matches well with the measured density but the floating potential prediction is several volts low. The +1-sigma IRI-2001 electron temperature at hour 1.5 matches the NLP measured values and coincides with the agreement between the maximum in the measured floating potential and the predicted value. In the equatorial region, PIM with the +1-sigma IRI-2001 is underestimating the measured floating potential and that is due to the measured electron temperature being lower than the model plasma input.

As noted earlier, the ISS configuration in August 2006 had the same PV array module and the same Russian segments as in 2001 when the GRC/FPP instrument acquired data. The core current collection components of PIM were developed against the GRC/FPP data set. The good comparison between the FPMU data and the present PIM predictions with appropriate IRI plasma input strongly suggest that PIM has correctly captured all of the elements of ISS current collection. The remaining step is to use the FPMU plasma data as input to PIM. Approval to do this is being worked through the ISS Program Environments Special Problems and Resolution Team.

4.2 - 2007/062 data

Figure 11 (on page 21) contains a summary plot of FPMU data and PIM predictions for an orbit in day 2007/062 and is presented in identical fashion as Fig.10. For early March 2007, the ISS orbit phasing had changed relative to day 2006/217 such that eclipse exit occurred at the maximum southern latitude. For the +XVV attitude and the starboard mounting of the FPMU, the $V_{ISS}xB\cdot\ell$ induced floating potentials are near zero for the southern hemisphere.

The agreement between the FPMU probes displayed in Fig. 11 is the same as that shown in Fig. 10. However, there appears to be a little more scatter in the WLP electron temperature data. The PIM prediction for eclipse exit floating potential with the -1-sigma IRI-2001 input matches well with the 15 V measured by the FPMU. The measured density and temperature mostly follow the -1-sigma IRI-2001 case. The predicted occurrence of the equatorial region charging is earlier

than the measurement due to the model temperature decreasing before hour 8.9 instead of after as indicated by the measured data.

Recall from Fig. 9 that the new PV array module has both wings deployed while only one wing remains deployed from the original PV array module. The fact that the measured plasma properties more or less coincide with the -1-sigma IRI-2001 case and the PIM prediction for this case matches the observed floating potential at eclipse exit strongly suggests that the collection properties of the new PV array are the same as the old array. Definitive proof awaits using the FPMU plasma data as input to PIM.

5 - SUMMARY

Since August 2006, the FPMU has been operated during several data sessions and is meeting its requirement of providing floating potential measurements of the ISS and its associated local ionospheric plasma. The FPMU measurements will be used for validation of the PIM, assessment of PV solar array manufacturing variability, interpreting/validating IRI-2001 predictions, and support plasma assessments of the ISS including forecasting. The FPMU interface with the video system accommodates a large amount of high-resolution data for each probe to be transferred each second of operation. This large amount of data allows filtering and smoothing techniques for data recovery that overcomes the noise in the data distribution path. Initial comparisons of FPMU data with the PIM model results indicate that the fundamental current collection characteristics for the ISS developed several years ago were appropriately captured. The initial results for the collection properties of the second PV array module activated in December 2006 indicate that they are consistent with the first PV array module installed in December 2000. For the limited cases examined here, the observed FPMU plasma data lies mainly within the ±1-sigma boundaries of the nominal IRI-2001 model prediction. Obviously there is fine structure observed in the real data that does not appear in the "climate averaged" IRI. Extending beyond the ISS needs, the FPMU is acquiring density and temperature data near the F2 peak that could contribute toward focused ionospheric physics studies, global model development, and/or calibration with other current satellite missions.

The FPMU will continue to operate during intermittent data campaigns for the remainder of 2007 and at least through 2008. Barring delays in the STS launch schedule, all four PV array modules should be integrated and operating in 2008.

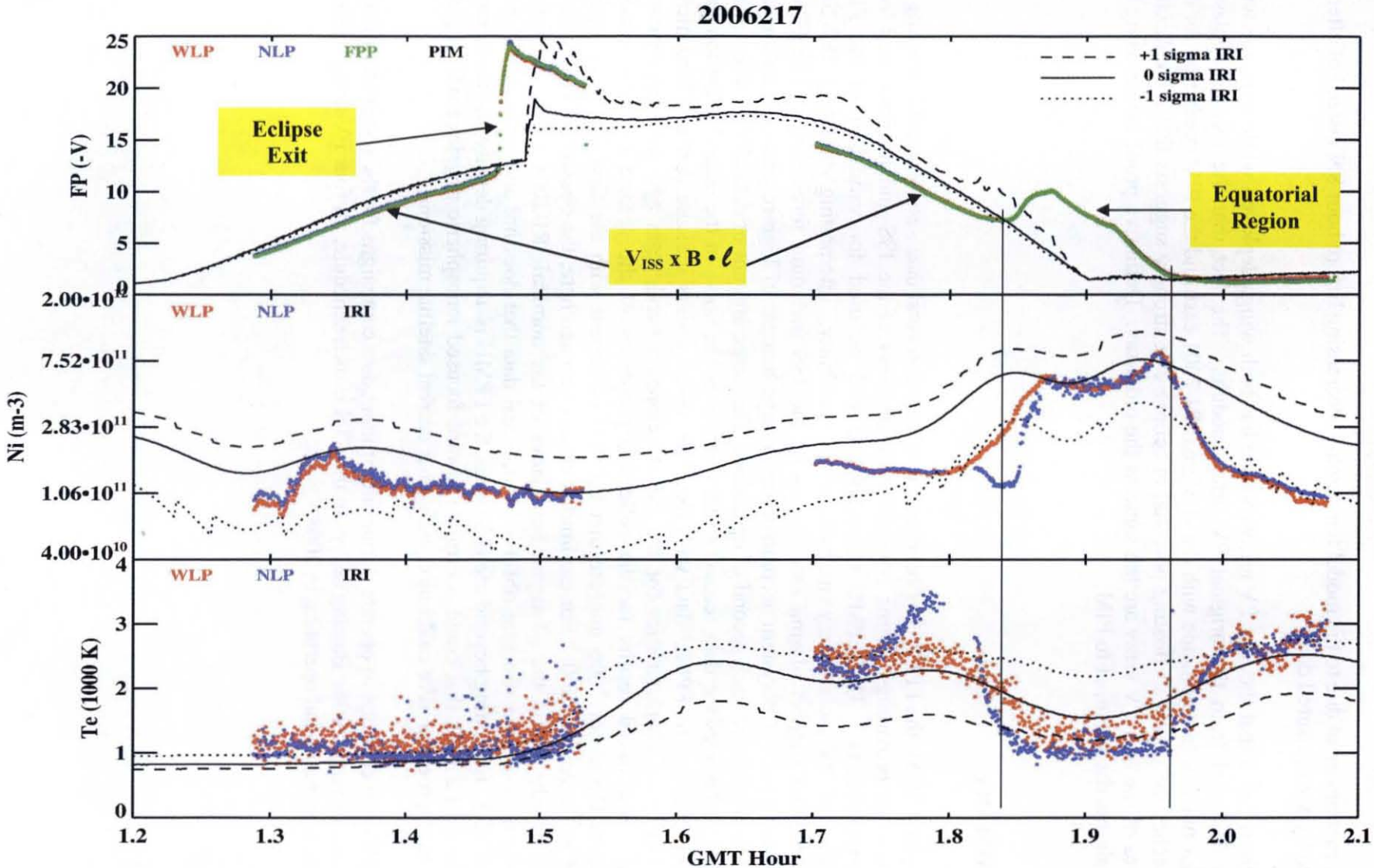

Figure 10 - FPMU data and PIM predictions for 2006/217/01:12 – 02:06.

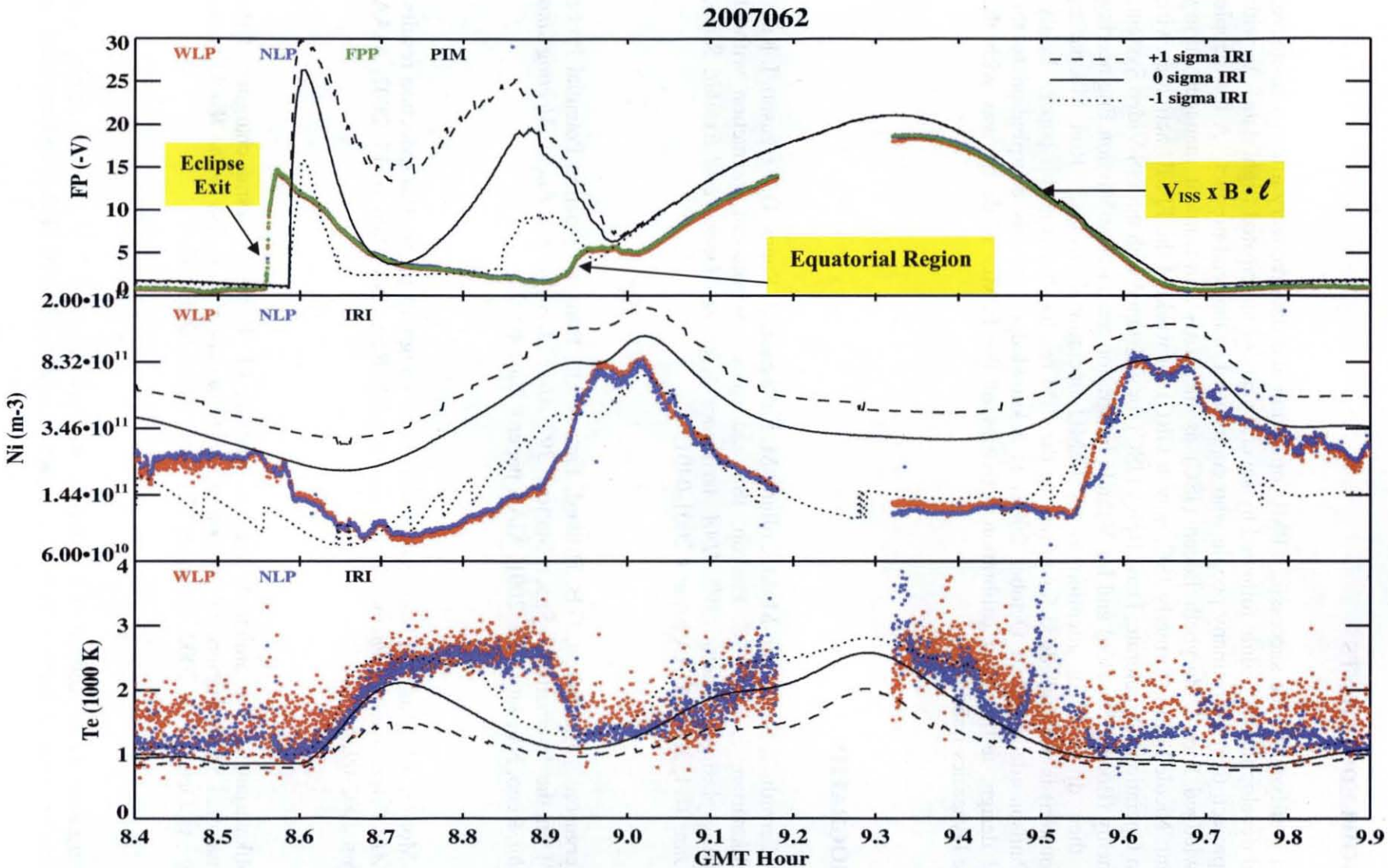

Figure 11 - FPMU data and PIM predictions for 2007/062/08:32 – 09:54.

6 - ACKNOWLEDGEMENTS

It is indeed gratifying to see successful FPMU operation and data recovery after an intensive, compressed development schedule followed by several years of anticipated flight data. As with any flight project, there were many people who contributed to that end product. A few people are acknowledged here: Marybeth Edeen (JSC) as the NASA instrument manager during development; Nicole Smith (formerly JSC, now at GRC) for working the FPMU activities with the Mission Operations Directorate; Dana Helvy (JSC) for assistance with the ISS Video System; and Jim Shelby (Boeing/Houston) and his Vehicle Integration team of the Mission Engineering Room for their diligence in attention to all FPMU operational details. Ron Mikatarian (Boeing/Houston) is acknowledged for providing the PIM results shown in this paper. Lastly, Brandon Paulson (deceased in October 2005) is acknowledged for his contribution to the mechanical design, testing, and calibration activities of the FPMU while he was with the USU/Space Dynamics Laboratory.

7 - BIBLIOGRAPHY

[1] M.R. Carruth, T. Schneider, M. McCollum, M. Finckenor, R. Suggs, D. Ferguson, I. Katz, R. Mikatarian, J. Alred, C. Pankop, ISS and space environment interaction without operating plasma contactor, *39th AIAA Aerospace Sciences Meeting and Exhibit*, Reno, NV, Jan. 9-11, 2001, AIAA paper # 2001-0401.

[2] D. Ferguson, T.L. Morton, G.B. Hilliard, First results from the Floating Potential Probe (FPP) on the International Space Station, *39th AIAA Aerospace Sciences Meeting and Exhibit*, Reno, NV, Jan. 9-11, 2001, AIAA paper # 2001-0402.

[3] T.L. Morton, J.I. Minow, Floating Potential Probe Langmuir probe data reduction results, *40th AIAA Aerospace Sciences Meeting and Exhibit*, Reno, NV, Jan. 14-17, 2002, AIAA paper # 2002-0936.

[4] R. Mikatarian, H. Barsamian, J. Kern, S. Koontz, J.F. Roussel, Plasma charging of the International Space Station, *53rd International Aeronautical Congress – The World Space Congress*, Oct. 10–19, 2002, Houston, TX, paper # IAC-02-T.2.05.

[5] D. Ferguson, G.B. Hilliard, T.L. Morton, R. Personen, ISS FPP electron density and temperature measurements – Results, comparison with the IRI-90 Model, and implications

for ISS charging, *41st AIAA Aerospace Sciences Meeting and Exhibit*, Reno, NV, Jan. 6-9, 2003, AIAA paper # 2003-1083.

[6] R. Mikatarian, H. Barsamian, J. Alred, J. Kern, J. Minow, S. Koontz, Electrical charging of the International Space Station, *41st AIAA Aerospace Sciences Meeting and Exhibit*, Reno, NV, Jan. 6-9, 2003, AIAA paper # 2003-1079.

[7] D.C. Ferguson, FPP results – final report, *10th Spacecraft Charging Technology Conference*, June 18 - 21, 2007, Biarritz, France.

[8] S. Koontz, M. Valentine, T. Keeping, M. Edeen, W. Spetch, P. Dalton, Assessment and control of spacecraft charging risks on the International Space Station, *8th Spacecraft Charging Technology Conference*, October 20-24, 2003, Huntsville, AL, NASA/CP-2004-213091.

[9] C.M. Swenson, D. Thompson, C. Fish, The Floating Potential Measurement Unit, *41st AIAA Aerospace Sciences Meeting and Exhibit*, Reno, NV, Jan. 6-9, 2003, AIAA paper # 2003-1081.

[10] C.M. Swenson, C. Fish, D. Thompson, Calibrating the Floating Potential Measurement Unit, 8th Spacecraft Charging Technology Conference, October 20-24, 2003, Huntsville, AL, NASA/CP-2004-213091.

[11] C. M. Swenson, D. Thompson, C. Fish, The ISS Floating Potential Measurement Unit, *9th Spacecraft Charging Technology Conference*, April 4-8, 2005, Tsukuba, Japan.

[12] J.P. Lebreton, S. Stverak, P. Travnicek, M. Maksimovic, D. Klinge, S. Merikallio, D. Lagoutte, B. Poirier, P.-L. Blelly, Z. Kozacek, M. Salaquarda, The ISL Langmuir probe experiment processing onboard DEMETER: Scientific objectives, description and first results, *Planet. Space Sci.*, *54*, 472-486, 2006.

[13] I. Katz, G.A. Jongeward, V.A. Davis, T.L. Morton, D.C. Ferguson, Current collection by a large Langmuir probe in a meso-thermal (ram) plasma, in *Measurement Techniques in*

Space Plasmas: Particles, eds. R. F. Pfaff, J. E. Borovsky, and D. T. Young, Geophysical Monograph 102, American Geophysical Union, 1998.

[14] L.W. Parker, B.L. Murphy, Potential buildup on an electron-emitting ionospheric satellite, *J. Geophys. Res.*, *72*, 1631, 1967.

[15] J. Rubinstein, J.G. Laframboise, Theory of a spherical probe in a collisionless magneto-plasma, *Phys. Fluids*, *25*, 1174, 1982.

[16] L.H. Brace, Langmuir probe measurements in the ionosphere, in *Measurement Techniques in Space Plasmas: Particles*, eds. R. F. Pfaff, J. E. Borovsky, and D. T. Young, Geophysical Monograph 102, American Geophysical Union, 1998.

[17] K. Balmain, The impedance of a short dipole antenna in a magnetoplasma, *IEEE Trans. Antennas Propagat.*, *AP-12*, 605, 1964.

[18] K. Balmain, Dipole admittance for magnetoplasma diagnostics, *IEEE Trans. Antennas Propagat.*, *AP-17*, 389, 1969.

[19] A. Barjatya, C. M. Swenson, Observations of triboelectric charging effects on Langmuir type probes in dusty plasma, *J. Geophys. Res.*, *111*, A10302, doi:10.1029/2006JA011806, 2006.

[20] J.C. Ward, C.M. Swenson, C. Furse, The impedance of a short dipole antenna in a magnetized plasma via a finite difference time domain model, *IEEE Trans. Antennas Propagat.*, *53*, 8, 2711- 2718, 2005.

[21] B. Reddell, J. Alred,, L. Kramer, R. Mikatarian, J. Minow, S. Koontz, Analysis of ISS plasma interaction, *44th AIAA Aerospace Sciences Meeting and Exhibit*, Reno, NV, Jan. 9-12, 2006, AIAA paper # 2006-865.

[22] T.A. Schneider, J.A. Vaughn, J.I. Minow, K. Hwang, K.H. Wright, B. Reddell, J. Alred, R. Mikatarian, P. Leung, S. Koontz, Current collection characteristics of International Space Station Russian thermal blanket material, *44th AIAA Aerospace Sciences Meeting and Exhibit*, Reno, NV, Jan. 9-12, 2006, AIAA-2006-0867.

[23] M.J. Mandell, V.A. Davis, B.M. Gardner, G.A. Jongeward, Electron collection by International Space Station solar arrays, *8th Spacecraft Charging Technology Conference*, October 20-24, 2003, Huntsville, AL, NASA/CP-2004-213091.

[24] H. Barsamian, R. Mikatarian, J. Alred, J. Minow, S. Koontz, ISS plasma interaction: measurements and modeling, *8th Spacecraft Charging Technology Conference*, October 20-24, 2003, Huntsville, AL, NASA/CP-2004-213091.

[25] D.C. Ferguson, T.L. Morton, An empirical model of ISS charging based on FPP and ODRC data of 04/11/01 through 04/13/01. Is shunting one array at dawn always a good EVA hazard control?", presentation to the ISS PCU Tiger Team, August 2, 2001.

[26] J.I. Minow, L.F. Neergaard, T.H. Bui, R.R. Mikatarian, H. Barsamian, S.L. Koontz, Specification of ISS plasma environment variability, *8th Spacecraft Charging Technology Conference,* October 20-24, 2003, Huntsville, AL, NASA/CP-2004-213091.

[27] J.I. Minow, Development and implementation of an ionospheric variability model, *Adv. Space Res.*, *33*, 887-892, 2004.

MSFC-292

Initial Results from the Floating Potential Measurement Unit aboard the International Space Station

K. Wright (UAH),

C. Swenson, D. Thompson, A. Barjatya (USU)

S. Koontz (NASA/JSC)

Todd Schneider, Jason Vaughn, Joe Minow,
Paul Craven, Victoria Coffey (NASA/MSFC)

Linda Parker (JE)

Them Bui (AA)

10th Spacecraft Charging and Technology Conference

June 18 - 21, 2007

Space Dynamics Laboratory
Utah State University Research Foundation

Background

- *Initial expectations of ISS charging were: 160V PV arrays with negative grounding + VxB•L + minimal conductuve area → high negative charging.*

- *To mitigate this, two Plasma Contactor Units were installed on ISS in 2000 ahead of the first PV array.*

- *Plasma diagnostic instrument (GRC/FPP) installed in December 2000 finds that the ISS does NOT charge as negative as predicted and the PCUs lower the magnitude of the charging.*

- *ISS charging model is developed by SAIC working with GRC. This model is further developed by SAIC for NASA working through Boeing and is now called the Plasma Interaction Model (PIM).*

Floating Potential Measurement Unit (FPMU)

- Follow-on instrument to GRC/FPP
- Developed by USU in 14 months
- Four probes providing redundant measurements

Role:

- Validation of PIM
- Assess PV array variability
- Interpreting IRI predictions

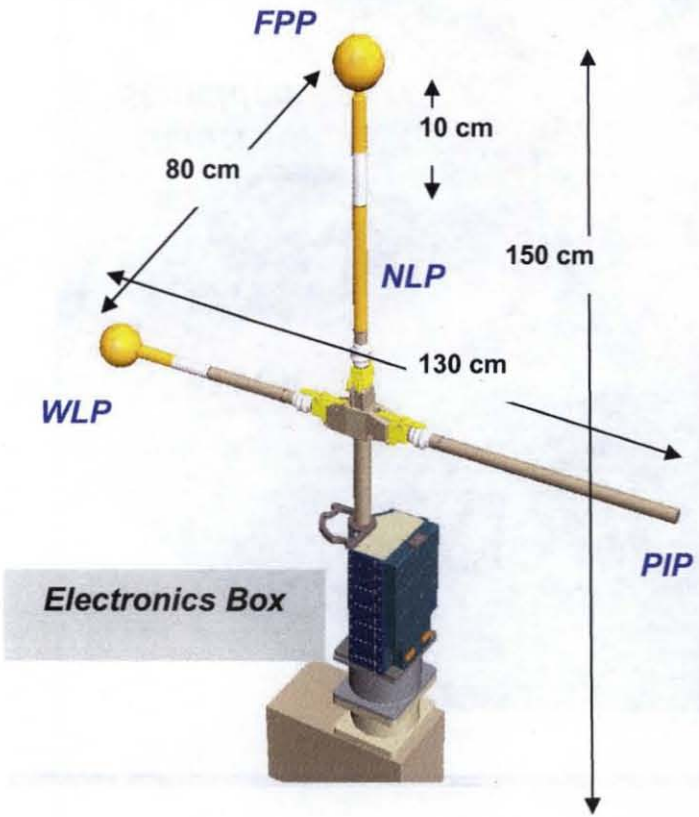

FPP: Floating Potential Probe
WLP: Wide-sweep Langmuir Probe
NLP: Narrow-sweep Langmuir Probe
PIP: Plasma Impedance Probe

Sensor	Measured Parameter	Rate (Hz)	Effective Range
FPP	V_F	128	-180 V to +180 V
WLP	N T_e V_F	1	10^9 m^{-3} to $5{\cdot}10^{12}$ m^{-3} 500 K to 3000 K -20 V to 80 V
NLP	N T_e V_F	1	10^9 m^{-3} to $5{\cdot}10^{12}$ m^{-3} 500 K to 3000 K -180V to +180 V
PIP	N	512	$1.1{\cdot}10^{10}$ m^{-3} to $4{\cdot}10^{12}$ m^{-3}

FPMU Operation

Year	GMT Day	Calendar Day
2006	215 - 220	Aug. 3 - 8
2007	022 - 030	Jan. 22 -30
	060 - 062	Mar. 1 - 3
	103 - 104	Apr. 13 -14
	123	May 3

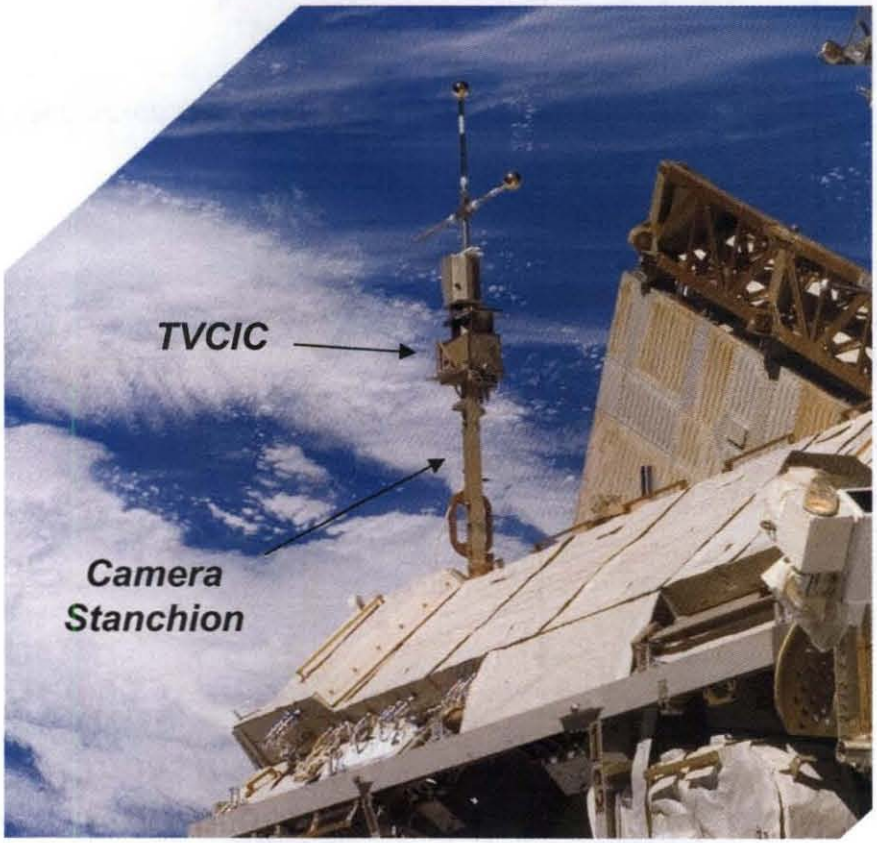

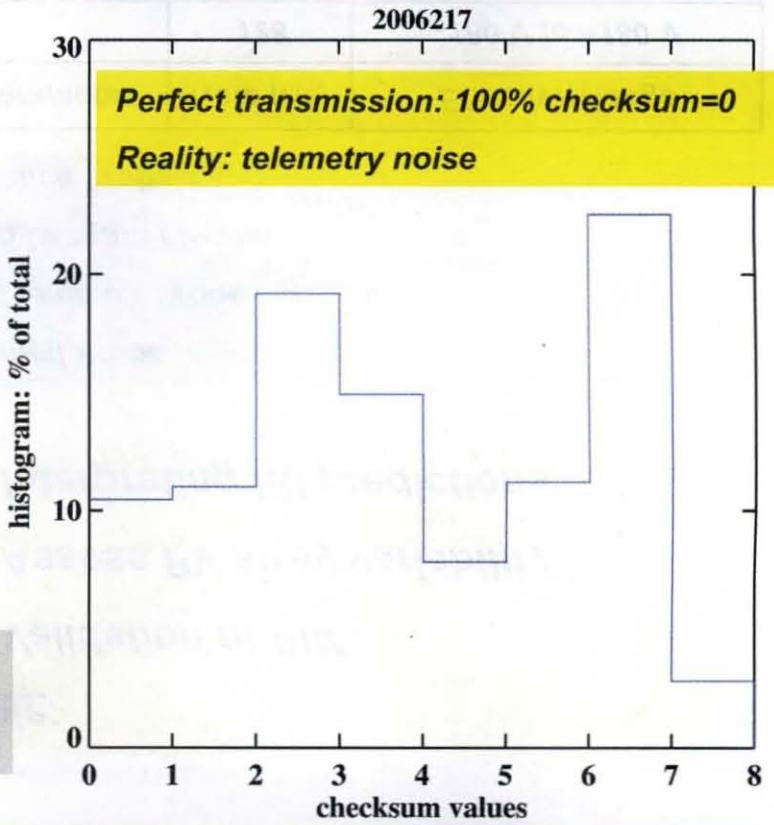

Camera interface provides high bandwidth →
6,776 16-bit words per one-second telemetry page!

FPP analysis method

Logic

- Select data only from $-10 \leq fpv \leq 150$
- Apply median filters
- Iterative process to exclude values > 2σ

Acceptance Criteria

- $|fp\_vdev/fpv| \leq 0.1$
- no. of surviving points ≥ 50

Recovery rates

> 98%

(> 90% for Jan 2007 Data Session)

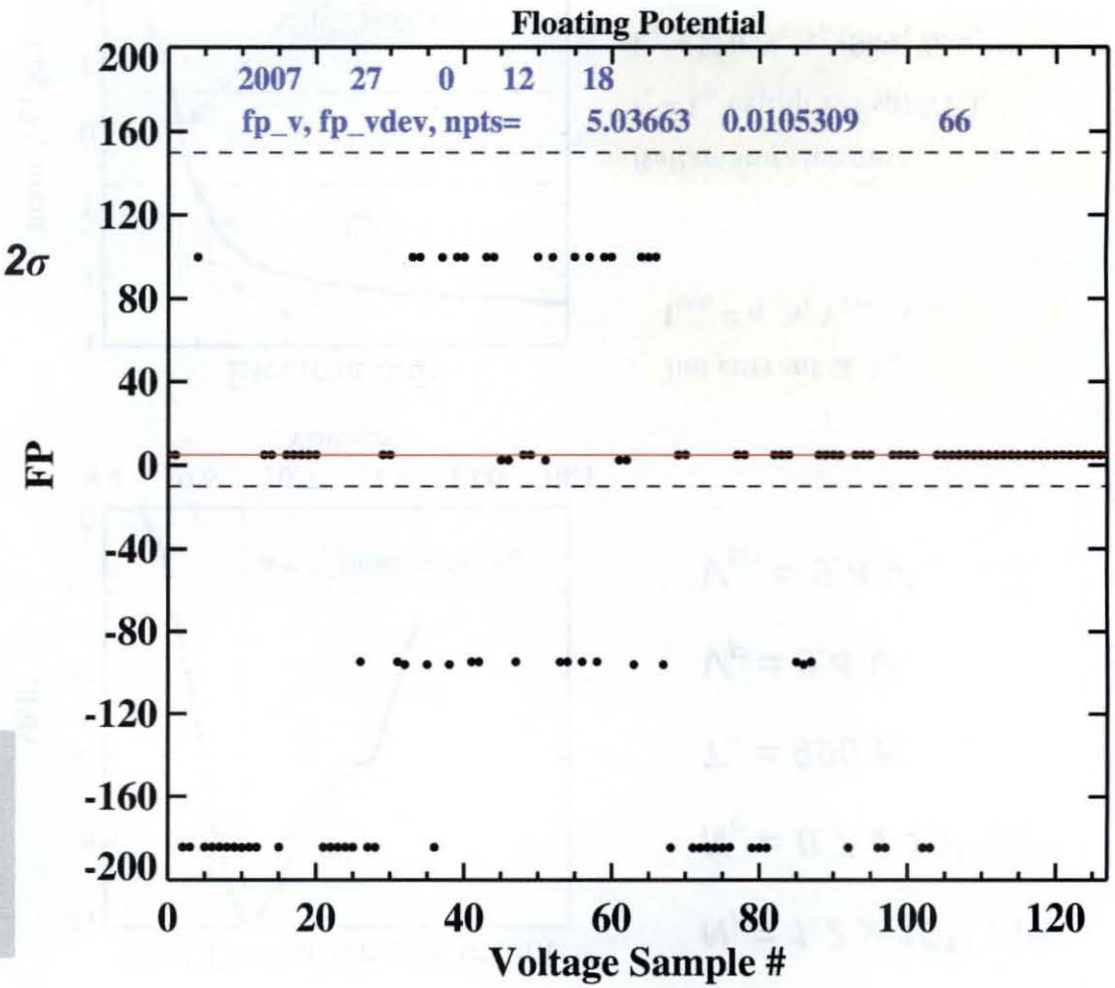

WLP analysis example: 2006/217/01:24:40

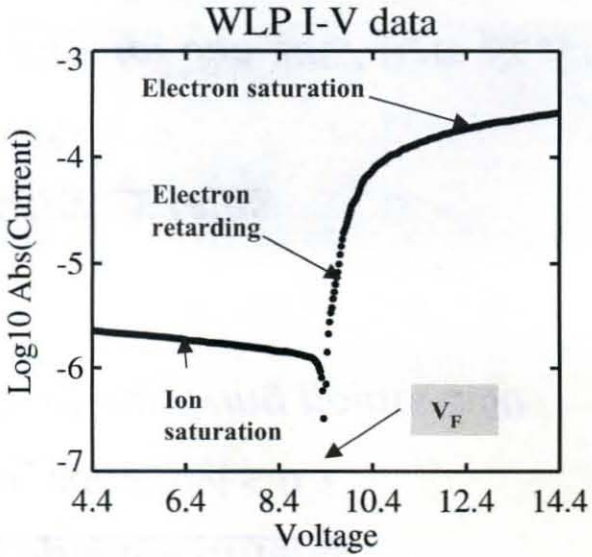

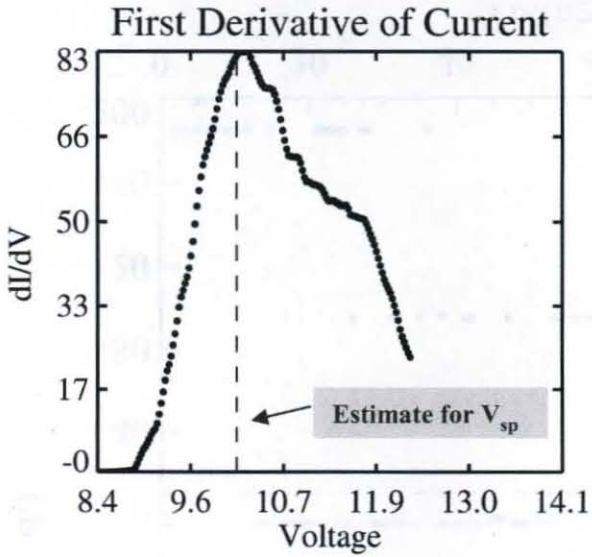

$N_i = 1.2 \times 10^{11}\ m^{-3}$

$N_e = 0.7 \times 10^{11}\ m^{-3}$

$T_e = 990\ K$

$V_F = 9.4\ V$

$V_{sp} = 9.8\ V$

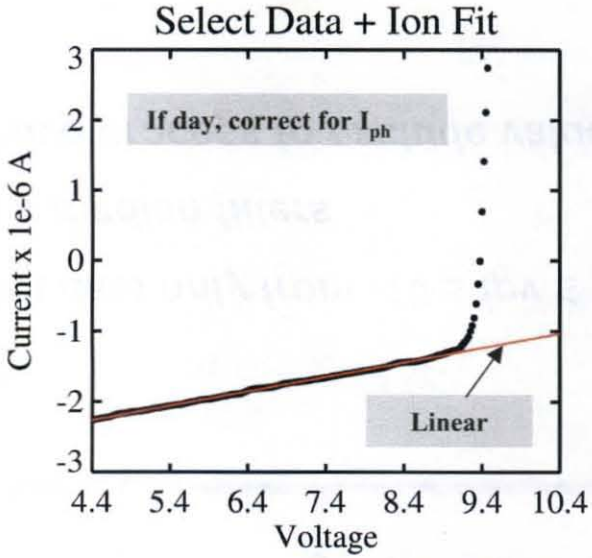

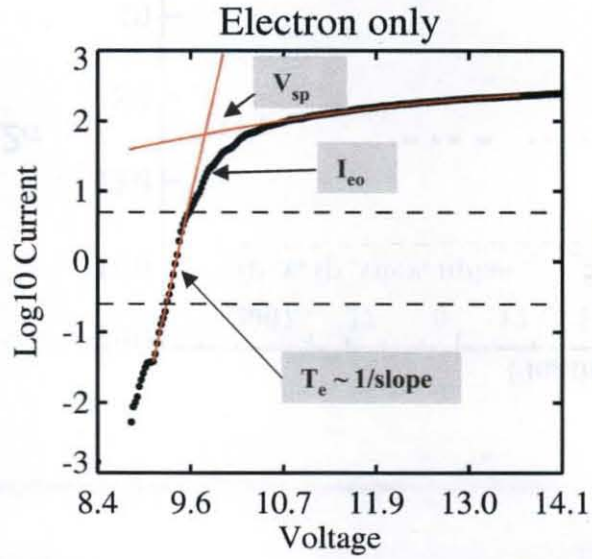

Ion current @ V_{sp}

$I_{ram} = q\ N_i\ V_{ISS} \cdot A_{LP}$

Boltzmann eletrons:

$I_e = I_{eo} \exp[q(V-Vsp)/kT_e]$,

$I_{eo} = \frac{1}{4}\ q\ N_e\ A_p\ (8kT_e/\pi m_e)^{1/2}$

NLP analysis example: 2006/217/01:24:40

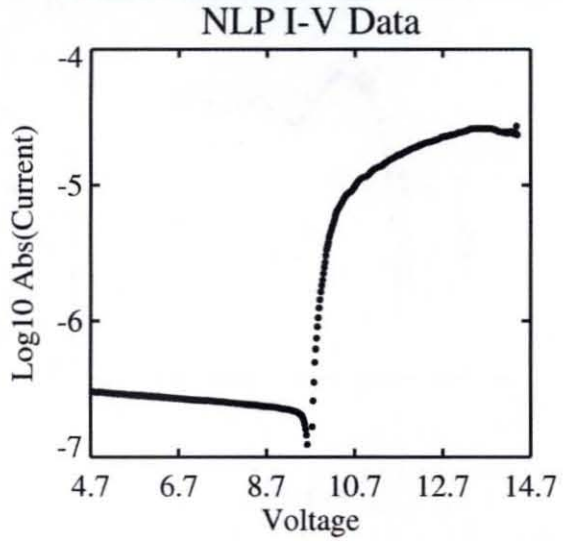

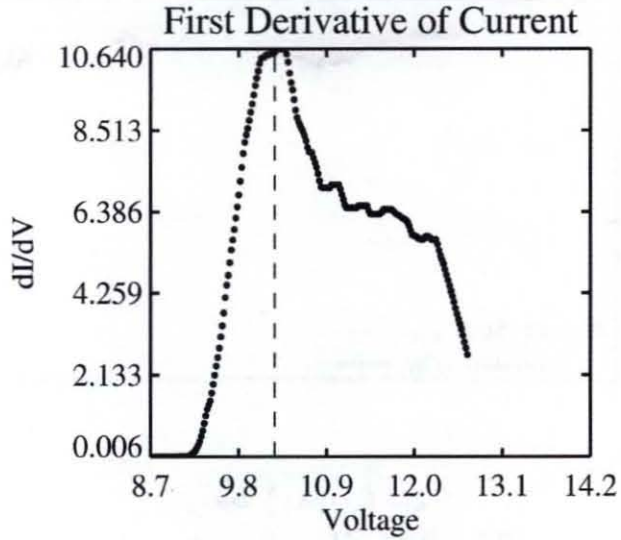

$N_i = 1.2 \times 10^{11}\ m^{-3}$

$N_e = 0.7 \times 10^{11}\ m^{-3}$

$T_e = 997\ K$

$V_F = 9.7\ V$

$V_{sp} = 10.0\ V$

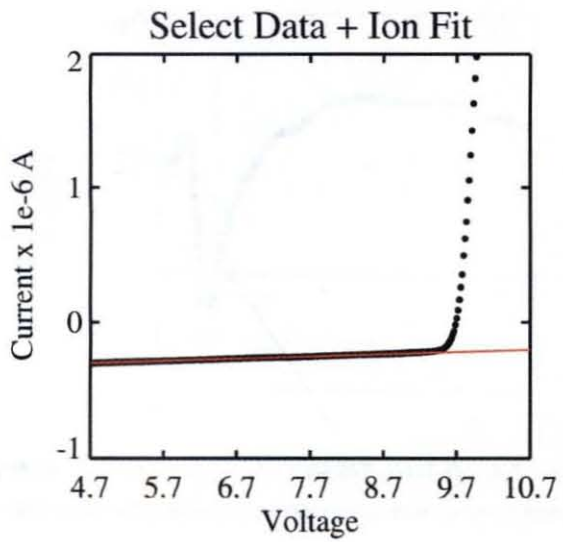

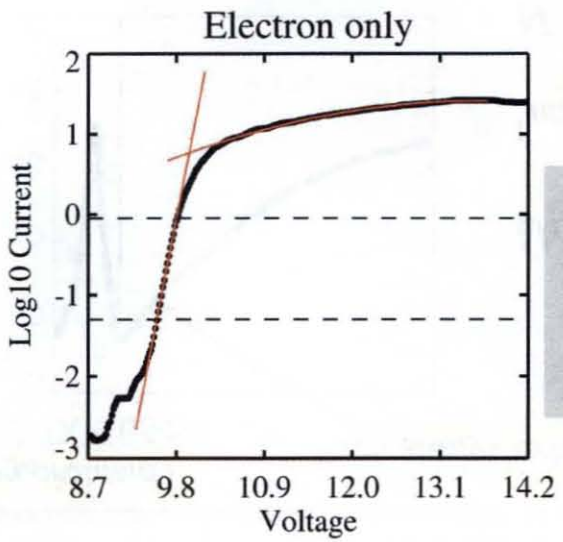

Analysis logic same as for WLP!

Only LP data from telemetry frames with checksum=4 accepted.

Recovery rates at 40% - 60%.

PIP analysis example: 2006/217/00:06:15

Phase behavior not consistent due to tracking problem !

Peak always exists!

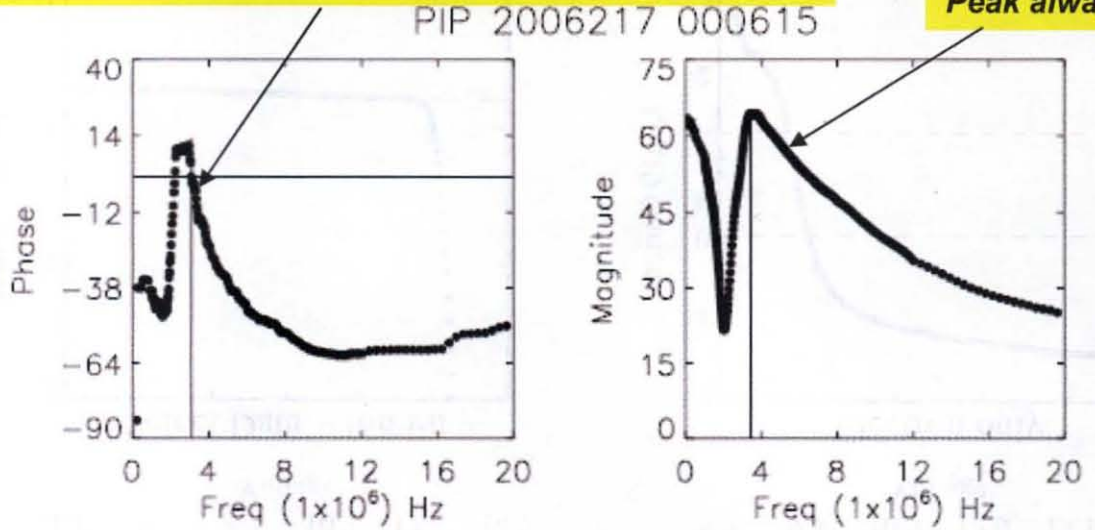

Upper hybrid resonance:

$$f_{uh}^2 = f_p^2 + f_c^2$$

$$N_e(m^{-3}) = 1.24 \times 10^{-2}[f_{uh}^2 - f_c^2]$$

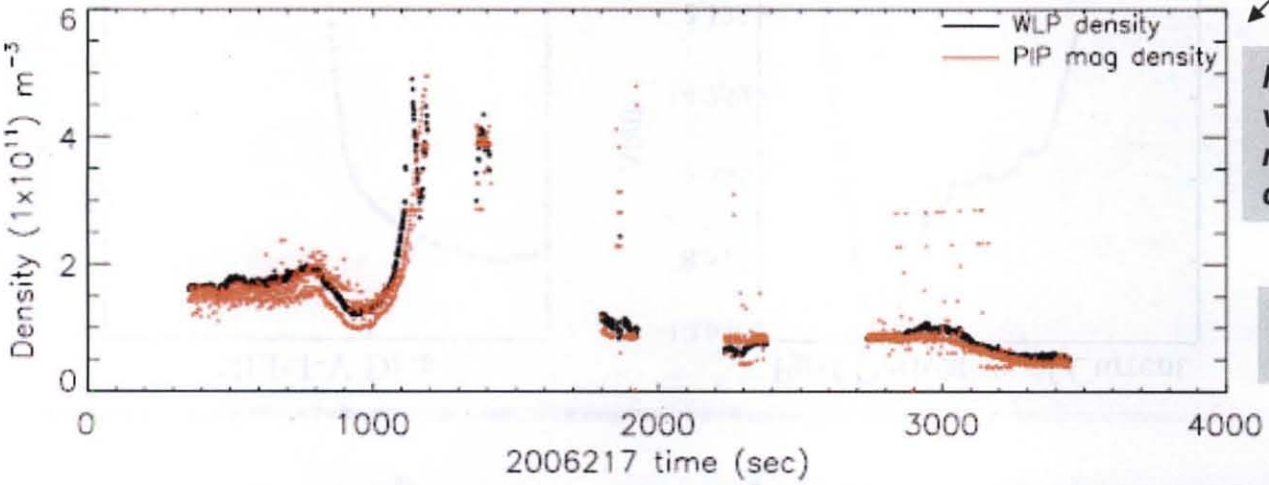

Note: For PIP data, all checksum values plotted – scatter can be reduced with only checksum ≤ 4 data.

Corroborates the further use of Ni from WLP and NLP.

2006/217: One PV array module
(same array as in the 2001 GRC/FPP data)

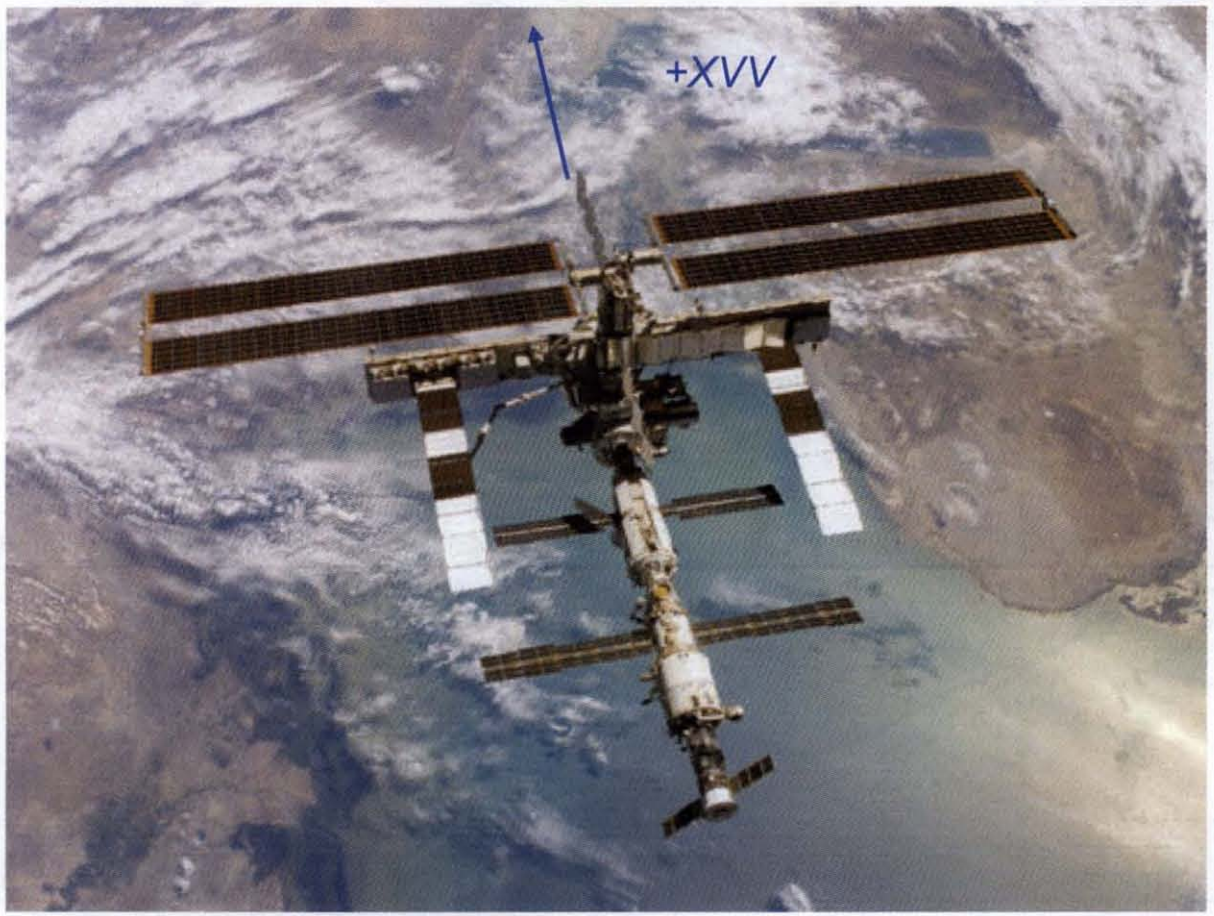

2006/217: One PV array module
(same array as in the 2001 GRC/FPP data)

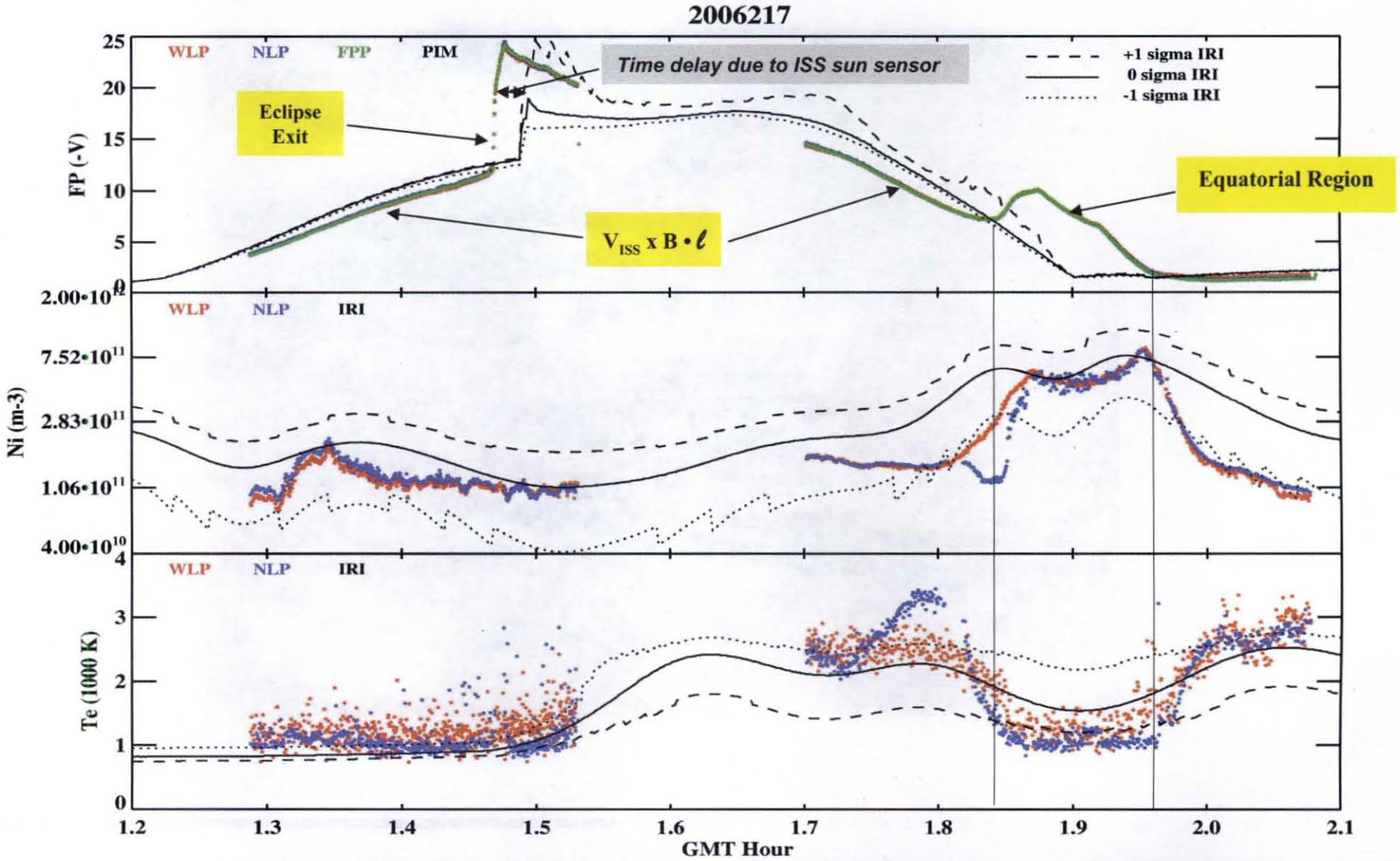

Variability of IRI-2001

- *Langmuir Probe data from AE-C, AE-D, and DE-2 collected*
- *Filtered for simultaneous N,Te pairs, ISS altitude and latitude for daylight*
- *For each measurement, the IRI-2001 value is determined*
- *From scatter plots, the ±1σ, ±2σ, and ±3σ boundaries are determined*

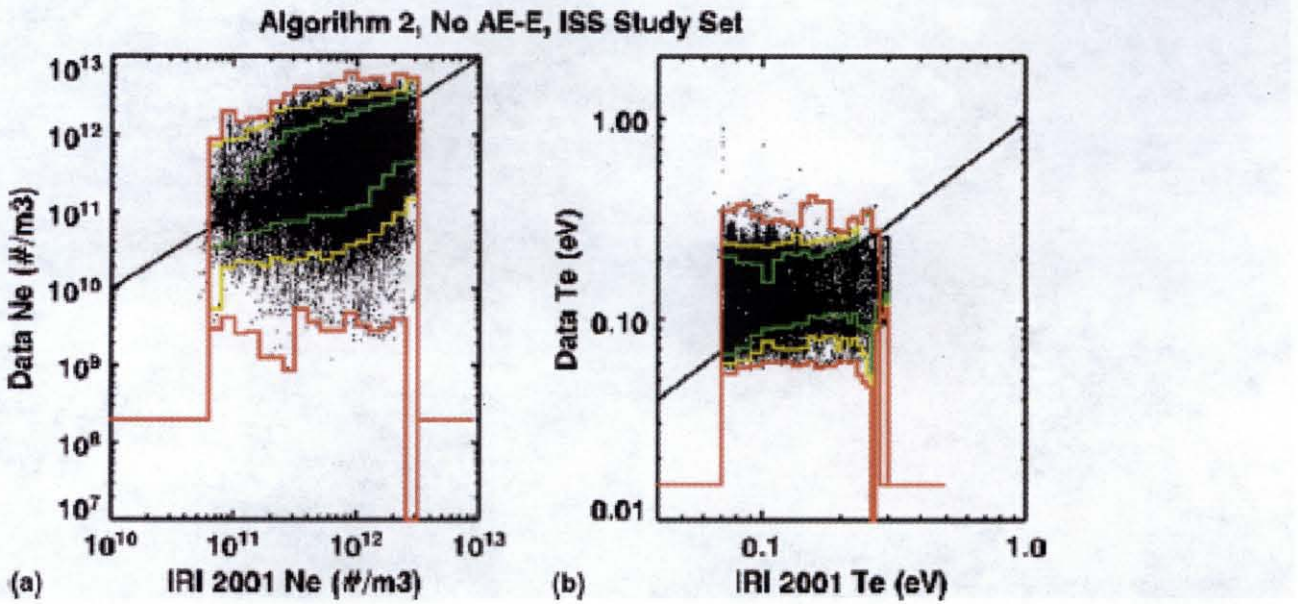

From Minow, Adv. Space Res., 33, 2004

2007/062: Two PV array modules
(only three wing sets operating, one folded)

2007/062: Two PV array modules
(only three wing sets operating, one folded)

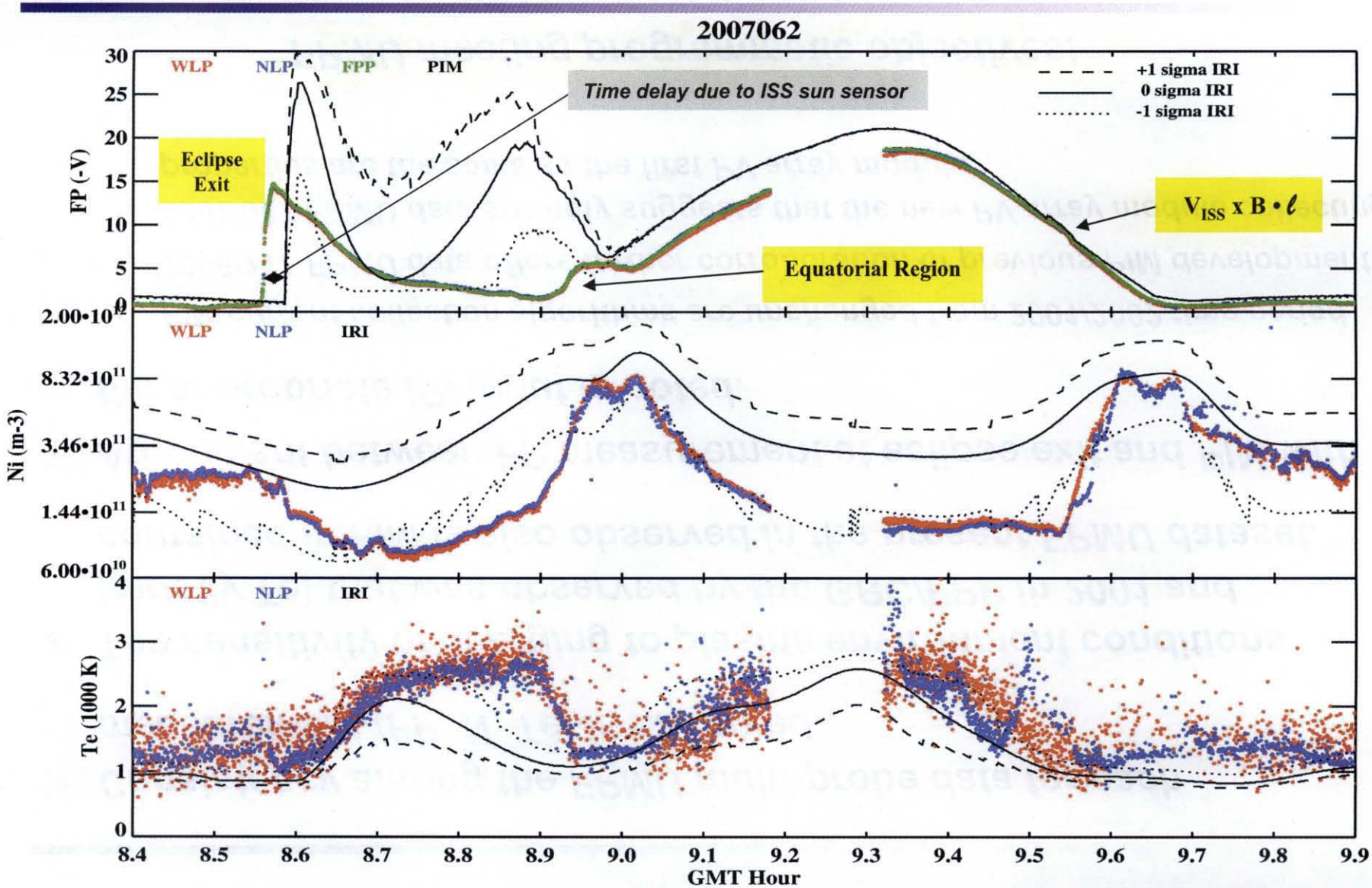

Summary

- Consistency among the FPMU multi-probe data for each measurement (FP, N, Te) is observed.
- The sensitivity of charging to plasma environment conditions (mostly Te) that was observed by the GRC/FPP in 2001 and contained in PIM is also observed in the present FPMU dataset.
- Agreement between FP measurement at eclipse exit and PIM with the appropriate IRI input is noted.
  - PIM current collection algorithms are unchanged from 2001/2002 time period
  - 2006/217 FPMU data offers further corroboration of previous PIM development
  - 2007/062 FPMU data strongly suggests that the new PV array module collecting properties are the same as the first PV array module.

FPMU meeting programmatic objectives!